Quaternary Geochronology 74 (2023) 101414

Contents lists available at ScienceDirect

Quaternary Geochronology

journal homepage: www.elsevier.com/locate/quageo

A universal approach to alpha-cellulose extraction for radiocarbon analysis of ^{14}C-free to post-bomb ages

Guaciara M. Santos [a,*], Anita S.Y. Komatsu [a], Jazmine M. Renteria Jr. [a], Arno F.N. Brandes [b], Christopher A. Leong [a], Silvana Collado-Fabbri [c], Ricardo De Pol-Holz [c]

[a] Department of Earth System Science, University of California Irvine, Irvine, CA, USA
[b] Instituto de Biologia, Universidade Federal Fluminense, Niterói, RJ, Brazil
[c] Centro de Investigación GAIA Antártica, Universidad de Magallanes, Punta Arenas, Chile

ARTICLE INFO

Keywords:
Resinous and parenchymatous woods
^{14}C-free wood
Bomb peak
Atmospheric ^{14}C calibration

ABSTRACT

In order to expand our in-house capabilities for tree-ring ^{14}C measurements in support of atmospheric ^{14}C reconstruction research, we designed a very versatile and inclusive procedure to produce high-quality α-cellulose homogenized extracts. The procedure can be easily scaled up or down (≤10 to 40 samples) and/or modified on demand (chemical steps can be easily adjusted to sample requirements as well, e.g., increased or diminished, according to the amount of available material and/or contaminants to be removed). Procedure setups are straightforward, and all products and instruments required are off-the-shelf. One to three days may be used to extract chipped wood to α-cellulose homogenized fibers that can be further used by high-precision ^{14}C accelerator mass spectrometry (AMS) analysis. The full procedure, which includes recommendations for wood reduction to chips, chemical treatment, and ^{14}C-AMS sample processing, measurements and data handling was tested on over 110 wood samples from post-bomb 1950AD to ^{14}C limit. Radiocarbon results were in the order of 0.29% or better, based on replication and regardless of the age group studied. Best background was in the order of 54 kyrs BP, without any type of background correction. Fourier transform infrared (FTIR) analysis was used as a characterizing tool to confirm the removal of unwanted carbon compounds during the production of α-cellulose extracts. For those analysis, we chose woods that are normally rich in resinous and parenchymatous structures. Results confirmed that our protocol produces pure α-cellulose extracts for ^{14}C analysis, and therefore this procedure can be safely applied to atmospheric ^{14}C reconstructions at pantropical regions.

1. Introduction

High-quality sampling and sample processing are the backbones of radiocarbon (^{14}C) age determinations. As instrumentation becomes more precise, sample handling for processing must be reevaluated and improved accordingly. Wood is a typical material used to constrain the ages of significant events (Danišík et al., 2012; Kutschera 2020), help to determine archeological site occupations (Jull et al., 2018), reinstate artifacts to their historical context (Ostapkowicz et al., 2012), and calibrate past and present ^{14}C atmospheric fluctuations over time (Hogg et al., 2020; Reimer et al., 2020; Hua et al., 2022). For wood to be measured in ^{14}C analyses, so that accurate results can be derived, it must be decontaminated from exogeneous carbon (i.e., carbon incorporated when samples were buried in geological and archeological settings) or taken to its most structural form, such as a cellulose-rich residual fraction (holocellulose and/or α-cellulose), since secondary carbohydrates and compounds may contain different isotopic signatures and ages (Hartmann and Trumbore 2016, and references therein).

For material within the sub-fossil ^{14}C range, Santos and Ormsby (2013) have shown that most of the so-called standard chemical treatment acid-base-acid (ABA), at different strengths and/or time durations, is quite suitable for reliable results, while circumventing wood loss during chemical dissolution. For samples at the ^{14}C limit (≫ 50 kyrs BP), these authors also showed that ABA protocols using 1N solutions and fewer intermediate steps (e.g., water rinses in between chemical treatments) tend to yield better results (in average 55kyrs BP, without background corrections). Findings were attributed to maximizing chemical efficiency while minimizing procedural-related contamination during sample treatment (procedural exogeneous carbon). Nonetheless, there are some circumstances in ^{14}C determinations (e.g., ^{14}C calibration

* Corresponding author.
E-mail address: gdossant@uci.edu (G.M. Santos).

https://doi.org/10.1016/j.quageo.2022.101414
Received 30 August 2022; Received in revised form 14 November 2022; Accepted 20 November 2022
Available online 25 November 2022

purposes; Reimer et al., 2020) where wood extractions to cellulose-rich residual fractions are required. Finding a procedure that can provide reliable results for the full ^{14}C age spectrum—i.e., from beyond 50 kyrs BP to post-bomb 1950 AD—is highly desirable.

Here, we present a user-friendly but efficient approach for extracting high-quality, high-purity α-cellulose microfibers from wood for ^{14}C accelerator mass spectrometry (AMS) analysis. The procedure uses the culture-tube setup (as sample treatment vessels) suggested by Southon and Magana (2010), couple with the minimized intermediated chemical steps evaluated by Santos and Ormsby (2013). The following steps of precise cutting of single tree ring woods (before chemical treatment), homogenization of α-cellulose fibers using an ultra-sonic bath, and drying microfibers on heat-block overnight (rather than using a freeze-drier) were added in this study, and then thoroughly evaluated for a course of a year. The entire procedure was assessed by replication using a large array of samples from the ^{14}C limit to post-bomb 1950 AD ages. Characterization of wood, wood extracts, and α-cellulose were carried out on selected samples by Fourier transform infrared (FTIR) as well as pre-extracted cellulose reference material. FTIR spectra concern to α-cellulose extract quality and are relevant for those wood samples derived from pantropical tree species, which are known to be very rich in extractives (Willför et al., 2003; Pinto et al., 2018), as well as parenchymatous structures containing mobile nonstructural carbon (Santos et al., 2022 and references therein).

2. Brief overview on wood chemical treatments and recent approaches for ^{14}C applications

For decades, mechanical and chemical pretreatments of wood and plant parts have been used to break down and remove undesirable carbohydrates and compounds from wood (e.g., extractives, hemicelluloses, and lignin). Alpha-cellulose extract, a chemically inert, cellulose-rich residual fraction of wood, has normally been chosen for isotopic and ^{14}C applications (Hajdas et al., 2017; Capano et al., 2018). This extract is generally obtained by a stepwise procedure that first targets soluble extractives with a series of organic solvents in a Soxhlet extractor (Hua et al., 2000), then targets lignin through acidified sodium chlorite (with acetic acid to help weaken lignin bonds), and finally targets hemicellulose through alkaline hydrolysis (Southon and Magana, 2010 and references therein).

The extractive holocellulose (α-cellulose and hemicelluloses) has also proven effective in ^{14}C analysis (Capano et al., 2018; Lange et al., 2019), including studies assessing tissue growth and/or dendrochronology dates confirmation. For instance, by measuring holocellulose from selected calendar years during the post-1950 AD period, stem growth tissue has been confirmed to be annual on pantropical tree species of *Entandrophragma utile* (Groenendijk et al., 2014), *Hymenolobium petraeum* (Linares et al., 2017), and *Polylepis tarapacana* (Ancapichún et al., 2021), along with *Araucariaceae* (Santos et al., 2015; Hadad et al., 2015) and *Cedrela* tree species (Baker et al., 2017).

Recently researchers have been 1) designing procedures in order to expedite chemical steps (see Gillespie (2019) 2ChlorOx procedure based on two cycles of alkaline hypochlorite followed by acidic chlorite oxidations, for example), or 2) evaluating existing chemical treatments (e.g., acid-base-acid (ABA), ABA-bleach (ABAB) or holocellulose, base-ABA-bleach (BABAB), 2ChlorOx, and α-cellulose) for their efficiency and reliability (Southon and Magana 2010; Santos and Ormsby 2013; Capano et al., 2018; Lange et al., 2019; Fogtmann-Schulz et al., 2021, Cercatillo et al., 2021). On these works pre-bomb woods of known ages and/or woods at the ^{14}C limit have been tested and reported. Where woods close to ^{14}C limit have been measured, ^{14}C-free results are sometimes reported after some type of background correction (Capano et al., 2018, Gillespie 2019). Therefore, they should be interpreted with caution when compared with other works in the literature. To some researchers, wood preservation levels seem to dictate the best chemical treatment to be applied (tough versus soft), so that enough product can be recovered for ^{14}C dating (Cercatillo et al., 2021; Susanne Lindauer, personal communication). While some agreed that the ABA or holocellulose fractions are reliable and less destructive (Southon and Magana 2010), and can also produce low ^{14}C-free results (Santos and Ormsby 2013; Lange et al., 2019), others still favor treatments that involves more delignification steps (Fogtmann-Schulz et al., 2021), especially when dealing with atmospheric ^{14}C reconstructions (Hua et al., 2022 and references therein).

The common prerequisite of treating wood with organic solvents (Hua et al., 2000) have been also under investigations. Organic solvents treatments can be applied via Soxhlet extractor on modes of single treatment (one sample per extractor; Hua and Barbetti 2004) or batch processing (multiple samples per extractor preloaded in sealed F57/41 Ankom filter bags; Gaudinski et al., 2005). Van der Wal (2021) used FTIR spectra and showed that cellulose-rich residual fractions from different protocols with or without the first solvent step treatments were basically identical, independent of the specific solvent protocol used (via Soxhlet extractor or single tube treatment with just acetone). With respect to post-bomb ^{14}C analysis of tree rings, works that had already abandoned the first solvent step treatment show no repercussions in the ^{14}C data, regardless of tree species (Hadad et al., 2015; Baker et al., 2017; Linares et al., 2017; Beramendi-Orosco et al., 2018; Santos et al., 2015, 2020, 2021; Ancapichún et al., 2021). Hence, organic solvent treatments do not seem to be essential, except under special circumstances (e.g., woods that undergo common conservation material; Dee et al., 2011). Sequential organic solvent treatments involving chloroform, petroleum ether, acetone, methanol, and water have been used to remove epoxy resin, paraffin, and unknown substances. However, there can be no guarantee of success, as aging, deterioration, or crosslinking may not remove preservative-treated wood substances completely (Brock et al., 2018).

During the breakdown to cellulose, acetic acid (CH_3CO_2H) added to acid-chlorite during the delignification of α-cellulose has also been tested for its impact on ^{14}C data. While Anchukaitis et al. (2008) have detected ^{14}C biases, Michczyńska et al. (2018) have reported that hydrochloric acid (HCl) treatment can reduce the risk of acetylation. This assessment has been confirmed even on single wood samples within the post-bomb age range. Santos et al. (2020) have shown that the 1N HCl treatment, typically used to avoid atmospheric CO_2 sequestration after the alkaline steps, can also help to reduce acetylation effects.

Streamlining protocols by adding semi-automated systems to handle time-consuming steps while increasing the number of wood samples processed per batch has been another recent approach to ^{14}C applications. Andreu-Hayles et al. (2019) have designed an α-cellulose extraction bath-apparatus with 150 funnels/samples consisting of glass tubes and borosilicate filters that can be assembled into polytetrafluoroethylene (PTFE) blocks, based on previous designs (e.g., Wieloch et al., 2011). The PTFE blocks allow for the drainage of chemicals from interconnected funnels, while extracts are kept secure. Whereas the initial bath-apparatus and chemical procedure was designed to produce cellulose extracts solely for stable isotopic analysis, it was later adapted and tested for ^{14}C analysis (Santos et al., 2020). Radiocarbon results from post-bomb to sub-fossil samples were accurate and precise, but background samples yielded unimpressive results. Averaged values from ^{14}C-free woods uncorrected by any background were $F^{14}C = 0.0071$ ($n = 6$), equivalent to 40 kyrs BP, making this procedure unsuitable for woods within the ^{14}C-limit. Similarly, Fogtmann-Schulz et al. (2021) reported an α-cellulose experimental setup containing 50 handcrafted glass vessels plumbed to a diagraph vacuum pump for waste chemical removal, and then immersed in a water bath for treatments. Chipped woods in individual vessels are placed on porous glass filters, which also retain the insoluble fraction while chemicals can pass through them freely. This system's ^{14}C performance was evaluated using wood samples in two specific timeframes (i.e., 1420 AD and background). Chemical treatments tested used small variations in chlorination and delignification steps. Overall ^{14}C results on a predated single ring from

1420 AD were excellent, regardless of treatment applied, while background value clustered around 47.5 kyrs BP ($F^{14}C = 0.0026$).

Summarizing the points above, we can say that i) the use of organic solvent treatments (Hua et al., 2000) seems mostly to be an unnecessary step that can be eliminated (Gillespie, 2019; Santos et al., 2021 and references therein) and/or reduced to special conditions (Ostapkowicz et al., 2012; Dee et al., 2020); ii) the usage of acetic acid as an enhancer in acid-chlorite during the delignification, another carbon-containing compound, can be circumvented by HCl treatment before neutralization and drying (Michczyńska et al., 2018; Santos et al., 2020). However, its complete elimination does not seem to significantly influence α-cellulose extraction quality and/or ^{14}C data (Santos et al., 2021); iii) most chemical procedure investigations have been used to preserve the material from specific ^{14}C age-ranges of interest (Cercatillo et al., 2021), or have emphasized improving or verifying best practices for woods within the ^{14}C limit (e.g., Southon and Magana, 2010, Santos and Ormsby, 2013, Hajdas et al., 2017; Gillespie, 2019; Michczyńska et al., 2018; Lange et al., 2019); iv) procedures that use semi-automated devices are attractive but do not seem to be able to yield very good results for woods at the ^{14}C limit (Santos et al., 2020; Fogtmann-Schulz et al., 2021). They also cannot possibly disregard the time consumed in pre-cleaning parts/items that need to be reused between batches. In addition, to make it worth the effort, they require a large number of samples per batch treated (Andreu-Hayles et al., 2019); and finally, v) any procedure or procedures that can make wood cleaning or cellulose-rich residual fraction extractions easier, faster, and more reliable for the full ^{14}C age spectrum is preferable.

3. Materials and methods

3.1. Sample selection

As a basis for this investigation, we selected materials with known ^{14}C values ranging from >55kyrs BP to post-1950 AD and consisting of several coarse wood samples and pre-extracted cellulose fibers. Samples came from known inter-comparison ^{14}C trials (i.e., the Fourth International Radiocarbon Inter-comparison [FIRI], and the International Atomic Energy Agency [IAEA]), while others were sub-fossil woods, in-house ^{14}C-free materials and holocellulose and parenchyma-rich wood leftovers from independent projects. All samples, including the pre-extracted cellulose fiber from FIRI, underwent the same chemical extraction procedure. A complete sample list and its rationale are given below.

- AVR07-PAL-37 (or AVR): This permafrost-preserved wood of >55 kyrs BP of *Picea* sp. from Yukon, Central Alaska, is frequently used as a blank to identify laboratory procedural contamination from several procedures, including extraction to cellulose fractions (Santos et al., 2020, 2021);
- AR2: This is a ^{14}C-free wood sample of rimu (*Dacrydium cupressinum*) collected from under a 4m-thick debris avalanche deposit from a coastal section of North Taranaki in New Zealand (Santos and Ormsby 2013). It has been routinely dated by liquid scintillation spectrometry at Waikato University since 2001 (Hogg, 2004), as well as at the Keck Carbon Cycle AMS (KCCAMS) facility at the University of California, Irvine (UCI) on some special projects, and more recently at the Centro de Investigación GAIA Antártica (CIGA), as a procedural blank in ^{14}C analyses;
- SR7269 (Two Creeks): Sub-fossil wood (*Picea* sp.) of 11,980 ± 30 yrs BP from buried bed forest in eastern Wisconsin, U.S., being used at KCCAMS/UCI as an internal laboratory standard for several years (Beverly et al., 2010);
- LEN013A set: Pre-bomb dendrochronological dated tree rings of a well-preserved *Fitzroya cupressoides* wedge from the Valdivian temperate forest on the west coast of southern South America (41°S), spanning from 910 BCE to 497 CE (Lara et al., 2020). These tree-ring samples are part of a larger ongoing project to extend the data-based span of the Southern Hemisphere ^{14}C calibration curve. Since those samples are designated for calibration purposes, wood material was sampled at a 5-year resolution (i.e., each sample represents five elapsed calendar years). Five wood samples were selected from this collection according to their material quantity so that duplicates or triplicates could be produced to evaluate accuracy/precision.
- FIRI-F: This is the whole wood of a Belfast pine (*Pinus sylvestris* L.) selected from an absolutely-dated master chronology. Uncalibrated ^{14}C age yields 4508 ± 3 yrs BP (3239-3200 BC), and has been used regularly as a secondary standard by several laboratories (Scott et al., 2019);
- FIRI-I: This is the cellulose component of a Belfast pine (*Pinus sylvestris* L.) ^{14}C dated to 4485 ± 5 yrs BP (3299–3257 BC; Scott et al., 2019). Though this sample has been synthesized to cellulose before release to laboratories, it was selected here to be subjected to the same chemical extraction method as the wood materials analyzed;
- FIRI-H: This is a German Oak (*Quercus robur* L. or *Q. petraea M.*) identified as Pettstadt 262, and belonging to a tree-ring master chronology (Spurk et al., 1998; Scott et al., 2004). The wood has been ^{14}C dated to 2232 ± 5 yrs BP (313–294 BC; Scott et al., 2019). It has also been frequently used at KCCAMS/UCI as an internal laboratory secondary standard (Beverly et al., 2010);
- FIRI-J: This modern mashed barley represents the grain growth in 1998 with a consensus value of 110.7 ± 0.04 pMC (Scott et al., 2004), and has been successfully used in inter-calibration studies and post-bomb projects (Santos et al., 2020, 2021);
- HP-samples: Post-1950 AD single tree rings dated by dendrochronological techniques of *Hymenolobium petraeum* tree species from Central Equatorial Amazon (1°S, 56°W) (Santos et al., 2022) (Fig. 1). This tree species contains an abundant amount of parenchymatous structures (Santos et al., 2022 and references therein), cell tissues known for storing water, carbohydrates, lipids, and several other compounds (Plavcová and Jansen 2015; Morris et al., 2016). Its wood material belonging to a larger project for reconstructing atmospheric post-bomb ^{14}C within the tropical low-pressure belt (TLPB), where data is still lacking (Santos et al., 2020, 2022). Eleven single tree rings, spread out between 1950 and 1990 and with enough material to produce replicates, were selected for testing.
- IAEA-C3: This is a cellulose extract from a single growing season from approximately 40-year-old Swedish trees. Material was processed to cellulose from raw wood at a paper factory in Burgum, Netherlands, and later handled by the Centre for Isotope Research CIO at the University of Groningen (Mook and Van der Plicht 1999). While those paper-like cellulose sheets are normally used by ^{14}C laboratories as reference material, it was used here as cellulose reference for FTIR analysis instead.

3.2. Sample handling and ^{14}C measurements

3.2.1. Wood cutting

To promote wood accessibility to chemical treatments, wood is normally reduced to smaller particles (e.g., powder or chips). We chose to work with wood chips to avoid material loss, especially when dealing with single whole tree rings. Centrifugation before pipetting solutions can be completely avoided, which drastically reduces the time it takes to move between chemical steps. Material lost during solution aspiration using a fine-tip pipette can also be eliminated.

Before reduction to wood chips took place, single whole tree-ring samples were inspected under a microscope to ensure that equivalent parts of early and late wood were included per sample analyzed. Wood sections were then reduced to chips of approximately 0.06 × 1.0 cm over surface-glazed ceramic crucibles (Fig. 2) using an ultra-sharp pair of clippers (e.g., a 0.9 cm opening jaw wire flush cutter). Recovery rates during wood cutting were also closely monitored (for more details, see the video - termed S1 - in the supplementary data), so that the tree rings'

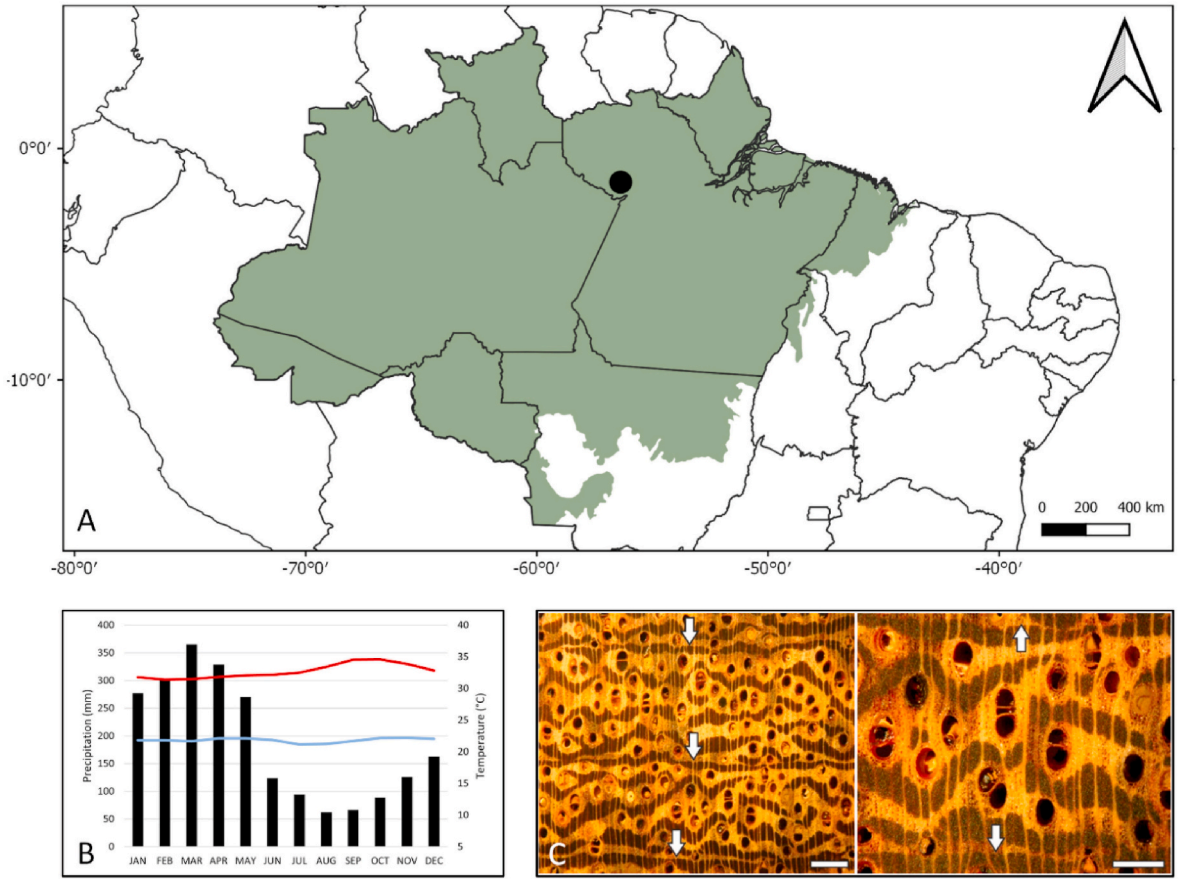

Fig. 1. *Hymenolobium petraeum* tree species information. A - Sampling location at Central Equatorial Amazon (1°S, 56°W). B - Ombrothermic diagram based on meteorological data recorded by a local industry (Mineração Rio do Norte) over the period 1971–1997 (bars = precipitation, blue line = minimum temperature, and red line = maximum temperature). C - cross-section view detailing anatomical features: e.g., marginal axial parenchyma delimiting tree rings (left), and paratracheal axial confluent parenchyma structures between tree ring boundary delimitations (right) (arrows indicate marginal parenchyma).

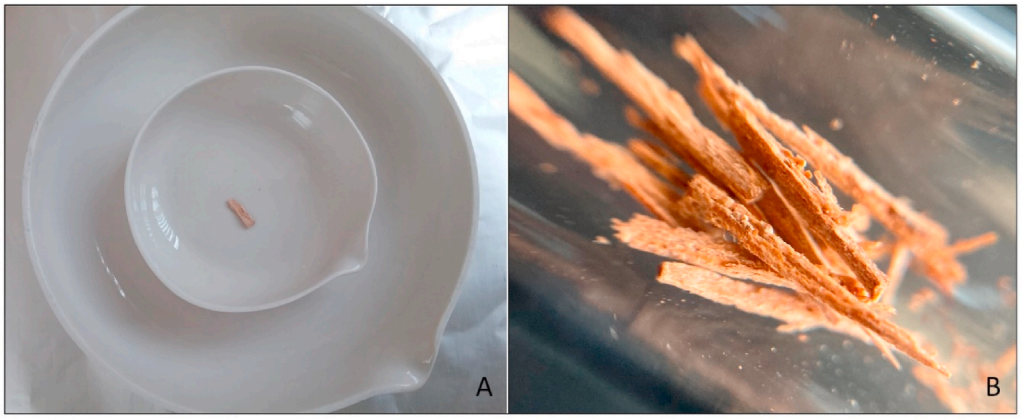

Fig. 2. Woodcutting strategy. A - Stacking up two dishes of different sizes ensures maximum-efficiency recovery during wood cutting. B - Upon wood weighing and recording, sample can be reduced to desired sizes. Samples are then reweighed, and their percentage recovery can be calculated.

full growing season could be preserved and recorded. Both procedures are relevant to avoiding ^{14}C bias, especially during the rising and falling portions of the bomb peak (i.e., between 1955 and 1970), and if tree rings analyzed are intended for calibration purposes (Santos et al., 2021, 2022). Percentage recovery rates during reduction to chips were 97% or better.

Other wood samples that do not pose undue concern, such as sub-fossil and ^{14}C-free woods used as secondary standards, microscope inspections, and/or monitoring of recovery rates during cutting, can be disregarded altogether. As our overall α-cellulose procedure has a recovery yield of approximately 30%, based on previous analysis, sample weights to produce one or multiple targets ranged from 11 to 30 mg. For ^{14}C-free samples (AVR and AR2) and FIRI-J barley, for which recovery tended to be lower (≤10%), treatment started with 25 or 40 mg maximum.

3.2.2. *Chemical treatment*

Chemical treatments of wood chips started by cycling 1N HCl and

NaOH at 70 °C until a clear supernatant was reached. This treatment is the same as the acid-base-acid (ABA) procedure described in Santos and Ormsby (2013). Next, a bleaching step with 1N HCl-$NaClO_2$ at 70 °C was employed for 3 h maximum (similar to that in Southon and Magana 2010). The procedure was carried out in a standard chemical fume hood to avoid exposure to irritating vapors. When the bubbling reaction ceased and wood chips appeared white, the supernatant was aspirated, and solids rinsed by 1N HCl. Alpha-cellulose was obtained next by immersing the holocellulose extract into 17.5% NaOH for 1 h at room temperature. To remove air-CO_2 captured during the NaOH treatment, the latter step was followed by 1N HCl at 70 °C. Alpha-cellulose extracts were then rinsed by ultrapure water at 60–70 °C to pH neutral and homogenized into microfibers with the help of an ultrasonic bath sonicator. Finally, cellulose fibers were allowed to settle, and once the final water rinse was aspirated, the loose fibers were dried overnight on a heat block set between 60 and 70 °C.

The chemicals, equipment, and accessories required to carry out this protocol are mostly off-the-shelf items that are commercially available (some recommendations can be found in Santos and Xu, 2017). The most-used chemicals in our procedure, 1N NaOH and HCl solutions, were purchased as ready-made chemical solutions from Fisherbrand (Fisher Scientific International, Inc.; 1N/certified SS266-1 NaOH and SA484 HCl). Other solutions—$NaClO_2$ and 17% (w/v) NaOH—were freshly prepared by dissolving solids (i.e., AA1426536 sodium chlorite, 80% technical grade and S3128-500 sodium hydroxide pellets (≥97%) from Fisher Scientific International, Inc.) in pure water, and in sufficient volume for a single treatment. For woody sample chemical treatments, sonication of final extracts to microfibers, drying, and storage, borosilicate glass 13 × 100 mm disposable culture tubes pre-baked at 550 °C were employed. Apart from making cross-contamination difficult, the use of a single test tube per sample during the entire treatment through to storage makes loss of material unlikely, as in this procedure insoluble material transfer during steps is not required. Ventilated plastic caps for plain-end glass culture tubes were used for closure during chemical treatments. To separate solids from the supernatant during chemical treatments, 5.0 ml disposable fine-tip plastic pipettes were used. A single pipette-aid per sample treated was used for the entire procedure: i.e., once the filtered suspension is aspirated and dispensed in a plastic waste container, labeled pipettes were ready to be reused in the following step. They can be rested upright in a second pre-designated, pre-baked culture tube placed in a test tube rack. In this way plastic pipettes are also sterilized during chemical treatments until the procedure is complete. For fiber homogenization, a 40 khz ultrasonic bath (Branson Ultrasonic Cleaner Timer CPX-952) was employed, and when necessary pre-baked disposable glass pipettes were used to poke and break down stubborn fiber buds into microfibers as well. For solution heating and sample drying, a scientific-type 150 °C dial benchtop heater (VWR® Analog Dry 2-Block Heaters) was used. After uncapped samples dried overnight under an aluminum foil tent, they were stored in their own plain-end glass culture tubes secured by leak-tight seal snap caps.

Since water rinses between chemical applications and the use of a centrifuge are not required (wood chips are too large to be aspirated), same-day wet α-cellulose extracts can be obtained from batches of ≤10 samples. For batches of >10 to 40 samples (maximum load on a single-dry heating system), the entire procedure can be accommodated in two or three days by using specific stopping points (e.g., after ABA, and/or after a bleaching step with 1N HCl-$NaClO_2$ at 70 °C and 1N HCl rinsing, if desired). Note that at the end of those steps, the final chemical solution used is always 1N HCl. In these cases, one should replace the 1N HCl solution by ultrapure water and let the mixture settle at room temperature overnight, until the procedure can be resumed the next day. The acidified mixture (solids and solution) prevents reabsorption of air-CO_2,

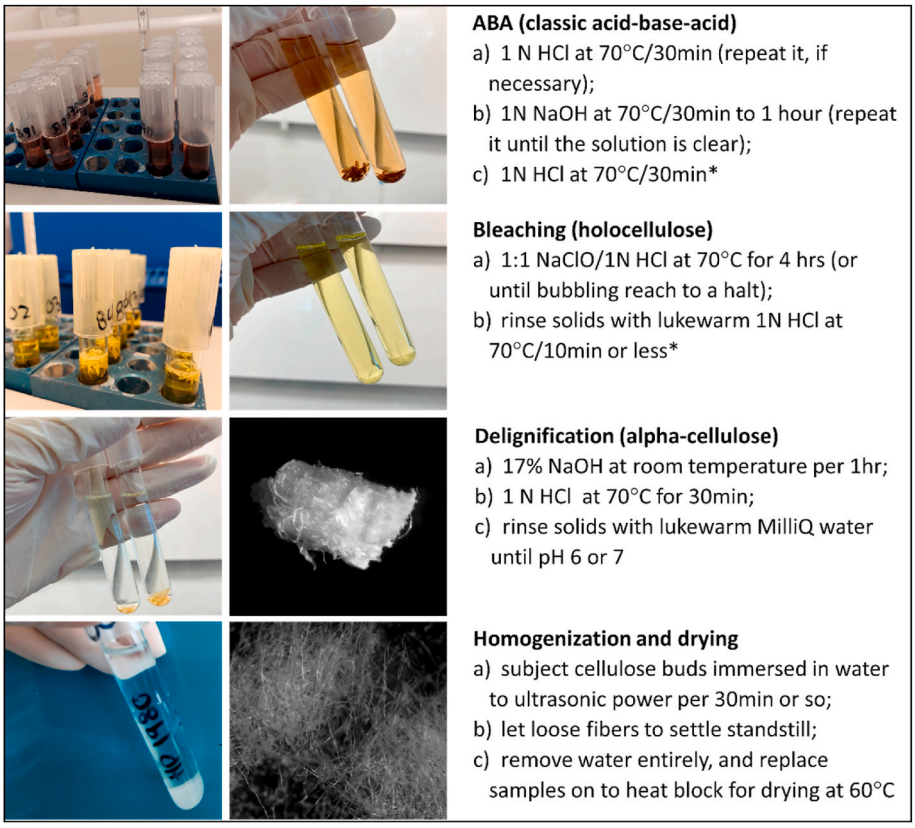

Fig. 3. Alpha-cellulose extraction process flow diagram. Asterisk (*) denotates the stopping points where sample extracts can be left overnight, once 1N HCl solution is replaced by MilliQ water. Keeping the solution at room temperature and at lower pH preserves solids from air-CO_2 contamination until the procedure can be resumed.

allowing solids to stay pristine. A process flow diagram (PFD) illustrating the steps and stopping points of this chemical procedure is shown in Fig. 3. Total recovery yield for the three main purification products (i.e., ABA, holocellulose, and α-cellulose fibril extracts) using the *H. Petraeum* samples as matrix are as follows: 69.0, 30.0, and 27.5%, respectively. Organic solvents were not employed here.

3.2.3. Radiocarbon measurements

Alpha-cellulose extracts were converted into carbon dioxide (CO_2) by combustion at 900 °C after transferring the microfibers (Fig. 3) into baked quartz tubes containing 40–50 mg of copper (II) oxide, tube evacuation, and sealing at the KCCAMS/UCI facility. For comparisons between different types of chemical extractions, the largest *F. cupressoides* (LEN013A-series) tree-ring sequences of the late Holocene were selected and divided into two sets. One set of wood samples underwent the isolation of holocellulose fibers at CIGA following Southon and Magana's (2010) protocol, thus excluding the use of a vacuum-dry device. The FIRI-I standards and AVR2 blanks were also processed to holocellulose at CIGA and sent to KCCAMS/UCI for further processing and ^{14}C-AMS analyses. The second set of wood samples of *F. cupressoides* (LEN013A-series) was shipped to the KCCAMS/UCI to undergo the procedure shown in Fig. 3. All organic combustibles evolved to CO_2 were later reduced to graphite over an iron powder catalyst following specific protocols (Santos and Xu, 2017). For normalization and quality assessment purposes, each wheel of cellulosic samples graphite targets was also loaded with 8 oxalic acid I (OX-I), one of each oxalic acid II (OX-II) from NIST, and sucrose from ANU graphite targets. Acid-base-acid USGS coal targets were also processed for ^{14}C-AMS analyses along with cellulosic samples. The latter were used to assess differences among sources of extraneous carbon from vacuum lines, graphitization reduction, and spectrometer performance versus α-cellulose chemical extractions.

Radiocarbon measurements were taken on a modified compact AMS system with ^{13}C/^{12}C measurement capabilities (NEC 0.5MV1.5SDH-1) to allow for online δ^{13}C-AMS isotopic-fractionation corrections (Beverly et al., 2010). Accuracy and precision based on replicates of OX-II (n = 18) and ANU (n = 18) reference materials were better than 0.29%. Reported ^{14}C results are shown as F^{14}C (i.e., fraction of modern carbon, defined as the ratio of the sample's radioactivity to the modern standard's radioactivity [Reimer et al., 2004]), and were obtained after fractionation and background corrections using calculations from Stuiver and Polach (1977).

3.2.4. Stable isotope analysis

To verify the homogeneity of α-cellulose bundles, three extracts from the 11 *H. petraeum* tree ring calendar years selected with sufficient material to be analyzed in duplicates were weighed out into 5 × 9 mm tin capsules (Costech Analytical Technologies Inc., Valencia, CA, U.S.) using a microbalance (Sartorius AG, Göttingen, Germany). Their associated calendar years are 1956, 1960, and 1970.

Total C content and stable C isotope ratio (^{13}C) were obtained using a Fisons NA-1500NC elemental analyzer (EA) equipped with a Thermo Finnigan Delta Plus stable isotope mass spectrometer (IRMS). The δ^{13}C results were measured as the ratio of the heavier isotope to the lighter isotope (^{13}C/^{12}C), and reported as δ values in parts per 1000 or per mil (‰) related to the Vienna Pee Dee Belemnite (VPDB) international standard. Accuracy/precision of 0.01% was attained on recognized EA-IRMS (e.g., USGS24 and atropine, $C_{17}H_{23}NO_3$) and in-house standards.

3.2.5. Fourier transform infrared spectroscopy (FTIR) analysis

FTIR spectroscopy of wood and wood extracts was employed to attain visual information on the structure of wood constituents and chemical changes taking place in woods that are suspected to contain substantial amounts of parenchymatous structures with mobile carbon, which have been reported to bias ^{14}C data (Santos et al., 2022).

To evaluate chemical steps, a batch of *H. petraeum* wood particles of ≤250 μm was produced from mixed tree rings with the help of an electrical grinder (Thomas Scientific 3383-L10 Laboratory Wiley Mini Mill Grinder) with a 60-mesh delivery tube. Other samples evaluated are the remaining cellulose fibrils produced originally from single tree rings reduced to chips from this study and others with similar objectives (i.e., produce high-quality α-cellulose extracts for ^{14}C analysis), and the cellulose inter-comparison material IAEA-C3.

The FTIR analysis spectra were obtained at the Laser Spectroscopy Labs, University of California, Irvine, with a JASCO FT/IR-4700 spectrometer set to a spectral range of 4000 to 400 cm-1 (wavelengths 2.5–25 μm), as standard conditions for all measurements.

4. Results and discussion

Wheels of cellulosic samples containing a large spectrum of chemically pretreated woody standards with distinct ^{14}C ages were produced and analyzed at KCCAMS/UCI. Since ^{14}C data accuracy and precision can be affected by instrument optimum conditions, ^{14}C measurements were made over widespread timepoints over a year. Hence, several wheels and ion-source cleaning conditions were employed. For simplicity's sake, ^{14}C results will be shown in sets following an ascending order (i.e., sorted from blanks and sub-fossil dates to post-bomb values). In this study, a total of 117 radiocarbon results of α-cellulose, 18 of holocellulose, and 18 of ABA (USGS coal, reference ^{14}C-free material used as combustion/graphitization blank, also uncorrected) are being reported on plots (Figs. 4–7) and Table 1. Radiocarbon values presented in plots (Figs. 4–7) are shown as deviations of the individual F^{14}C values of graphite targets measured from their F^{14}C weighted mean ($\Delta F^{14}C = F^{14}C_{meas} - F^{14}C_{wm}$) from replicates. Weighted mean values are displayed in each plot for easy viewing as well as their associated propagated uncertainty and number of replicates.

4.1. Results from ^{14}C-free samples

The performance of samples with ^{14}C ages beyond 55 kyrs BP is shown in Fig. 4. Radiocarbon results are shown as deviations to the weighted mean of ABA USGS coal targets. The ^{14}C weighted mean of both ABA USGS coal and α-cellulose AVR were virtually the same, e.g., 0.0018 ± 0.0004 (n = 18) and 0.0018 ± 0.0005 (n = 20), respectively. The best ^{14}C results for coal and AVR samples were 53,280 ± 280 and 54,030 ± 280 yrs BP, respectively, while unimpressive ones were 47,400 ± 340 and 46,260 ± 400 yrs BP. Note that this data has not been altered by background corrections of any kind, and it does reflect ion-source usage conditions over time.

Comparison of ^{14}C-free AR2 wood processed to α-cellulose and holocellulose, calculated similarly to those samples shown above, are also displayed in Fig. 4. Their weighted average F^{14}C yielded slightly higher averaged values: i.e., 0.0024 ± 0.0007 (n = 4; equivalent to 50,080 yrs BP) for α-cellulose and 0.0028 ± 0.0007 (n = 5; equivalent to 47,470 yrs BP) for holocellulose. Even though α-cellulose ^{14}C results seem superior and on-target, holocellulose results are within ±2σ of them.

In general, our α-cellulose ^{14}C data indicates that this straightforward procedure is effective for ^{14}C-free samples. Moreover, and to a large extent, this simple and quicker procedure yielded better results than those in previous studies found in the literature and presented above. While it is almost impossible to infer which of several causes is the most plausible for the ^{14}C blank variability detected here (Fig. 4), one cannot disregard the spectrometer contributions. Nonetheless, those small changes can be easily accounted for by regular measurements of ^{14}C-free samples, such as coal and chemically extracted wood.

4.2. Results from sub-fossil to late Holocene

In this study, four reference materials within the sub-fossil age range were processed and ^{14}C-AMS measured. Their ^{14}C ages vary from approximately 2-12 kyrs BP. Their ^{14}C results are shown in Fig. 5.

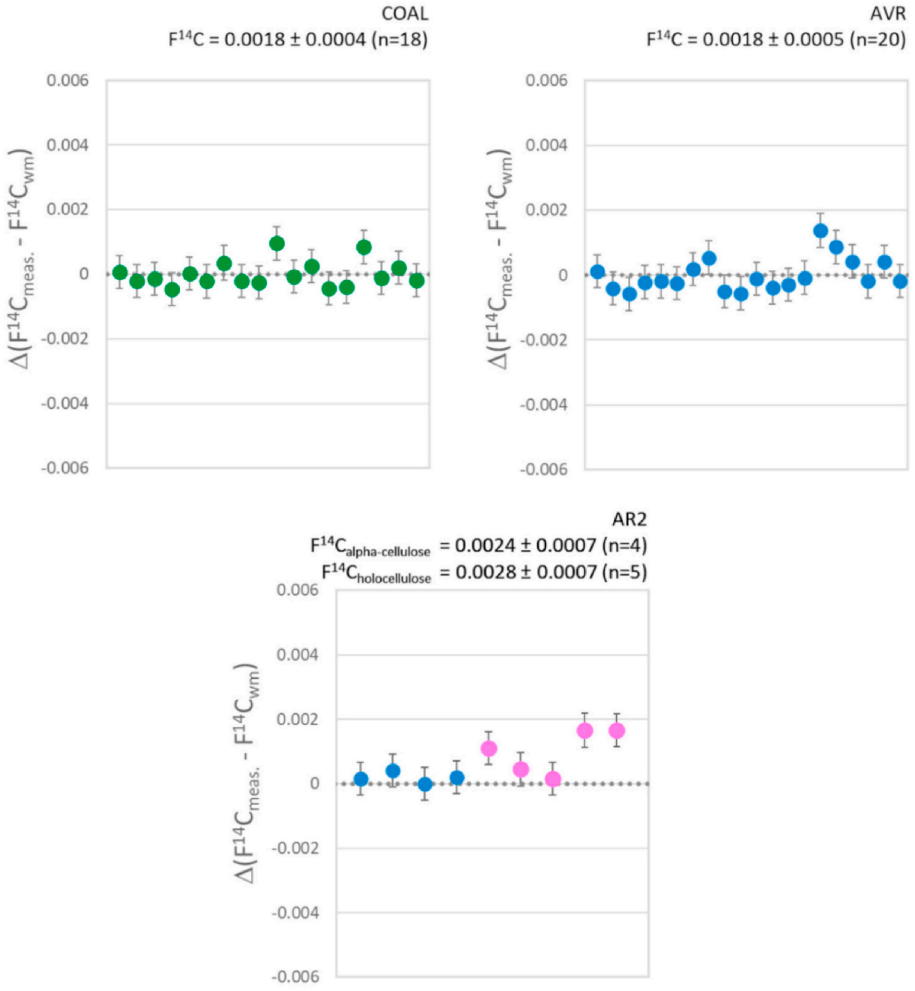

Fig. 4. Radiocarbon values for USGS Coal (green symbols for ABA), AVR (blue symbols for α-cellulose), and AR2 (blue symbols for α-cellulose and pink for holocellulose samples). For conformity, the $F^{14}C$ weighted mean used in calculations is from coal results (e.g., 0.0018 ± 0.0004).

Equivalent averaged ^{14}C ages are 11,981 ± 17 (n = 6) yrs BP for SR7269, 4516 ± 12 (n = 7) yrs BP for FIRI-F, 4488 ± 9 (n = 4) yrs BP for FIRI-I, and 2232 ± 10 (n = 9) yrs BP for FIRI-H. These ^{14}C ages are in excellent alignment with consensus-value ages reported elsewhere: i.e., Scott et al. (2004, 2019) and Beverly et al. (2010).

Overall, ^{14}C sample-to-sample variability was very small, regardless of their ^{14}C age range, sample processing, or measurement timing. FIRI-I, which is already found in cellulosic form, was subjected to two chemical treatments. While one cannot detect variations in accuracy among chemical treatments, again ^{14}C values from α-cellulose seem to be consistently on-target, and therefore more precise than those from holocellulose alone.

Radiocarbon results for the late Holocene LEN013A *F. cupressoides* series are shown in Table 1, as $Fm^{14}C$ and ^{14}C ages. Five sets of samples of five-year sequences were processed to α-cellulose and holocellulose. While it was not feasible to measure duplicates of both chemical treatments for each calendar year range, in all cases ^{14}C results overlap within ±2σ of each other, except for UCIAMS# 253,667, which appears slightly older than its counterpart replicates (i.e., holocellulose UCIAMS# 253,674 or α-cellulose UCIAMS# 255,230 fractions). Precision fitness was much higher among duplicates obtained from α-cellulose extracts than among those obtained from holocellulose, demonstrating once more that our α-cellulose treatment is equal to or better than other traditional cleaning methods (Southon and Magana 2010). Still, the standard deviation between pairs (regardless of chemical extract fraction) was better than the range/difference of the two data points plus uncertainties.

4.3. Results from post-bomb samples

Techniques used to determine the preliminary ring counting dates of *H. petraeum* tree species found at 1°S, 56°W have been reported elsewhere (Linares et al., 2017), followed by their annual frequency validation by ^{14}C. To examine atmospheric circulation patterns and local anthropogenic activities from the Central Brazilian Amazon, a full sequence of 63 single tree rings from 1938 to 2007 from this tree species/site has been recently measured by ^{14}C (122 results in total) and published in Santos et al. (2022), using interlaboratory α-cellulose extracts obtained from two laboratories. Here, we report isolated α-cellulose extracts from 11 pre-assigned calendar years spread over a range of 30 years that were subjected to the protocol summarized at the PFD (Fig. 3). Optimal matches between stem tissue growth (Dec–May) for the 11 calendrical dates and atmospheric post-1950 AD ^{14}C calibration curves of Southern Hemisphere (SH) Zone 3 bomb curves (Hua et al., 2013, 2022) were found and are displayed in Fig. 6.

For each calendar year measured in this study, 2–5 samples were processed, and ^{14}C-AMS targets were measured on multiple occasions. Radiocarbon results were similar at each instance, so symbols in Fig. 6 basically overlap each other. To better understand the results of these different tree rings/^{14}C data, we show the changes in $F^{14}C$ value of each calendar year as $\Delta F^{14}C$ in Fig. 7. Weighted mean $F^{14}C$ and propagated errors are also displayed. Remarkably precise results have been

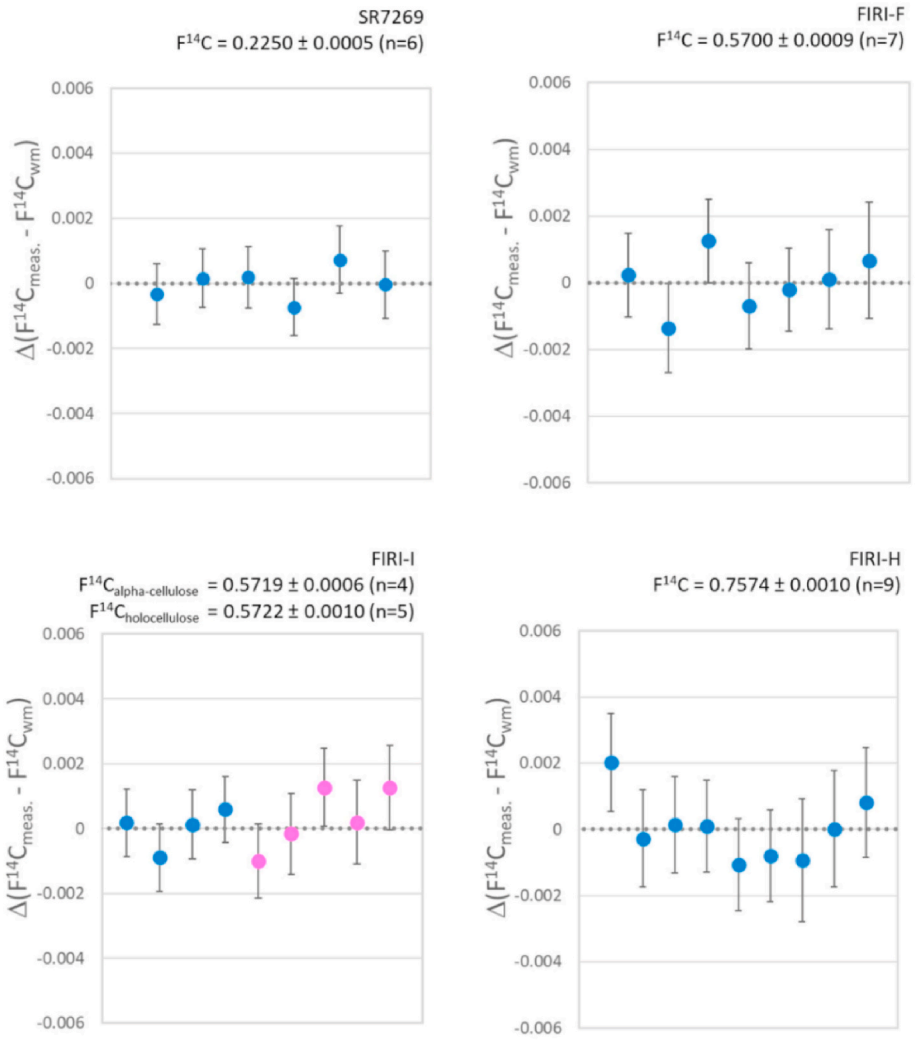

Fig. 5. Above are the ^{14}C values for four pre-bomb sub-fossil reference materials. For FIRI-I blue symbols denote α-cellulose, while pink denotes holocellulose extracts produced at CIGA.

obtained, regardless of timestamps measured.

Three calendar years (1956, 1960, and 1970) provided enough material for $\delta^{13}C$ analysis to be measured in duplication. Those calendar years were evaluated by stable C isotope ratio in order to confirm cellulose extract homogeneity. Their $\delta^{13}C$ averaged values are −25.1, −25.6, and −25.5‰, respectively. Estimating precision using duplicate measurements yielded ±0.01% or less, a standard deviation performance modestly better than that reported by Laumer et al. (2009). Equivalently, these results also illustrate the closeness between isotopic results, and therefore are another indicator of α-cellulose homogeneity precision. Twenty-five FIRI-J barley mash samples, a post-bomb reference material, were also processed alongside *H. petraeum* tree rings. Weighted mean $F^{14}C$ and propagated errors are displayed in Fig. 7, and they also overlapped with the consensus value reported in Scott et al. (2004). Due to the properties of natural barley mash, the FIRI-J broke down quickly in the α-cellulose chemical treatment and yielded roughly a 10% recovery.

4.4. Results from FTIR analysis

In line with other ^{14}C studies (Hajdas et al., 2017; Michczyńska et al., 2018; Fogtmann-Schulz et al., 2021; Van der Wal 2021), we utilized FTIR spectral differences in order to evaluate organic compound contents and removal after chemical treatments. We analyzed a tropical wood known to contain significant amounts of parenchymatous tissues and extractive compounds, and the effects of the main three chemical preparation steps we used to obtain homogenized α-cellulose fibers (i.e., ABA, bleaching/holocellulose, and delignification/α-cellulose). For this purpose, particles of ≤250 μm *H. petraeum* wood (Fig. 1) were ground, divided into three parts, and taken to the chemical extracts of interest, following the protocol in Fig. 3. An early aliquot of *H. petraeum* single tree ring extracted and homogenized to α-cellulose microfibers from chips was also analyzed. The resulting spectra are shown in Fig. 8.

This simple but helpful visual inspection of wood products after chemical processes by FTIR supports the effective removal of wood extractives, as well as other mobile carbon compounds of wood. *H. petraeum* wood original compounds were well identified by cellulose, lignin, hemicellulose, and extractives at the spectra of the corresponding untreated wood spectrum. No contamination can be seen surrounding the 1649 cm^{-1} resin peak area of final treated products (e.g., holocellulose and α-cellulose extracts). Many of the aromatic wood-based compounds shown in the untreated wood spectrum (in the region between 1600 and 1100 cm^{-1}) are still present after the ABA treatment. Our findings are similar to those of Michczyńska et al. (2018) when studying tree species of *Pinus sylvestris* L. from the Younger Dryas and Allerød period.

Resin peak and aromatic compounds have disappeared from the holocellulose and α-cellulose spectra (Fig. 8). In fact, very little

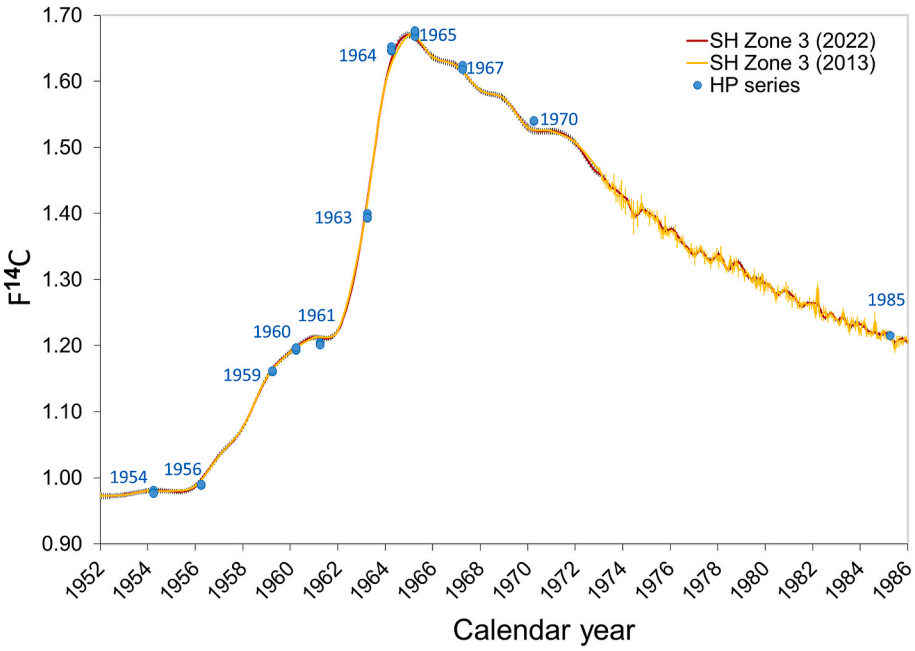

Fig. 6. The $F^{14}C$ post-bomb *H. petraeum* (HP) results for 11 selected calendar years are plotted in blue and compared to the SH Zone 3 compilations of Hua et al. (2013 and 2022). Calendar year AD points were adjusted to middle Dec–May, followed by a six-month uncertainty, based on precipitation information for the local growing season (Fig. 1), plus optimal matches between adjusted dendrochronological dates of the full record (1938–2007) shown in Santos et al. (2022) and atmospheric post-AD 1950 ^{14}C calibration curves.

difference can be observed between those chemical treatments. Both showed the typical bending vibrations of the C–H and C–O groups of the polysaccharides at 1330–1380 cm^{-1}, the C–O–C asymmetric stretching vibrations at the 1161 cm^{-1} range associated with cellulose I and cellulose II, and the peak intensities around 900 cm^{-1} attributed to interactions between glycosidic linkages and glucose units of the cellulose, as described in Aguayo et al. (2018). Still, the absorption peaks in the 1500-850 cm^{-1} region are slightly better defined from α-cellulose extracts than from the holocellulose, possibly due to delignification using NaOH treatment within 15–20 wt % at approximately 25 °C (Oh et al., 2005). It is unclear, however, if such small changes would bear distinct ^{14}C data, as we have not analyzed holocellulose aliquots of *H. petraeum* by ^{14}C in this study. Michczyńska et al. (2018) showed that insoluble constituents of holocellulose and α-cellulose of pine species are roughly similar in chemical composition by FTIR as well as ^{14}C analysis.

While *H. petraeum* α-cellulose extracts' FTIR spectra of both powder and chips (Fig. 8) support the full length of our protocol's delignification process (see Richard et al., 2014), we still prefer to use wood chips during sample chemical treatments. Wood chips helps on eliminate wood losses during solution aspiration, as well as helps to avoid centrifugation between chemical steps.

We also compared the FTIR of the remaining α-cellulose microfibers of the tropical tree species *H. petraeum* (this study and Santos et al., 2022), *Peltogyne paniculata* and *Cedrela fissilis* (Santos et al., 2021) against Belfast pine FIRI-F (*Pinus sylvestris* L.) using our extraction method (cf. Fig. 3). Cellulose IAEA-C3 standard, as it was distributed to labs, was used as reference. The resulting spectra from these comparisons are shown in Fig. 9 in the range of 800–4000 cm^{-1}, so that the absorbance peaks at the 3400–3300 cm^{-1} regions could be included as well. Those peaks are the stretching and bending vibrations of the OH and CH groups of cellulose (Oh et al., 2005; Aguayo et al., 2018). As shown in Fig. 9, the resulting spectra, which include all α-cellulose extracts from different tropical species (*H. petraeum, P. paniculata and C. fissilis*) plus Belfast pine (FIRI-F), show remarkable agreement with each other. They also agree with the well-known cellulose inter-comparison material IAEA-C3 extracted by others. All main peaks of cellulose are displayed, as well as the missing resin peak after chemical processing. The latter is crucial when dealing with post-bomb tree rings at annual resolution, as resins can become translocated within wood tissue. Note that the samples evaluated here are the remaining cellulose fibrils produced originally for this study and others with similar objectives (i.e., high-quality cellulose extracts for ^{14}C analysis; Figs. 4–7, and results reported in Santos et al., 2021).

Finally, even though wood materials from rings before 1954 were exhausted in the previous study (Santos et al., 2022), and were not retested here, previous results showed that our chemical protocol to produce α-cellulose completely removed transported metabolites between consecutive years. Otherwise, bomb-derived ^{14}C levels, transferred in pre-bomb wood, would show up and appear unusually elevated during this age-period (Stuiver and Quay 1981). The pre-bomb ^{14}C results of *H. petraeum* tree species shown in Santos et al. (2022) match with expected values, and reinforce the high quality of the α-cellulose extracts produced here.

4.5. The effectiveness of a versatile and inclusive α-cellulose procedure

Cellulose is an important component in plants' cell walls and is often separated from other compounds, such as hemicelluloses, lignin, and extractives, by chemical steps for it to be used in isotopic studies. Newly developed cellulose-rich residual fraction protocols have focused on boosting the number of extracts per batch when maintaining ^{14}C result reliability (Gillespie, 2019; Santos et al., 2020; Fogtmann-Schulz et al., 2021). However, due to the large array of ^{14}C dating ages, complete and thorough investigations on reducing contamination as well as increasing efficiency, accuracy, and precision tend to focus on specific ^{14}C age groups (the pre- or post-bomb timescale), effective ways to deal with woods within the ^{14}C limit, and/or levels of structural degradation (e.g., Southon and Magana, 2010, Santos and Ormsby, 2013, Hajdas et al., 2017; Gillespie, 2019; Michczyńska et al., 2018; Lange et al., 2019, Cercatillo et al., 2021). Thus far, a universal ^{14}C wood procedure has been deemed difficult to accomplish.

Hence, we developed an α-cellulose procedure for a large array of ^{14}C ages. The procedure's effectiveness has been demonstrated on multiple types of woody materials (e.g., ^{14}C-free and sub-fossil rimu, spruce, oak, pine, and post-bomb barley). But even more impressively, the procedure's accuracy and precision have been found using the Chilean long-lived conifer *F. cupressoides* (Table 1) and Amazon basin tropical parenchyma rich woods (*H. petraeum*, this study). Other Amazon Basin tropical trees, the deciduous tree species of *P. paniculata* and *C. fissilis* (Santos et al., 2021), were accurately measured as well. Many of those

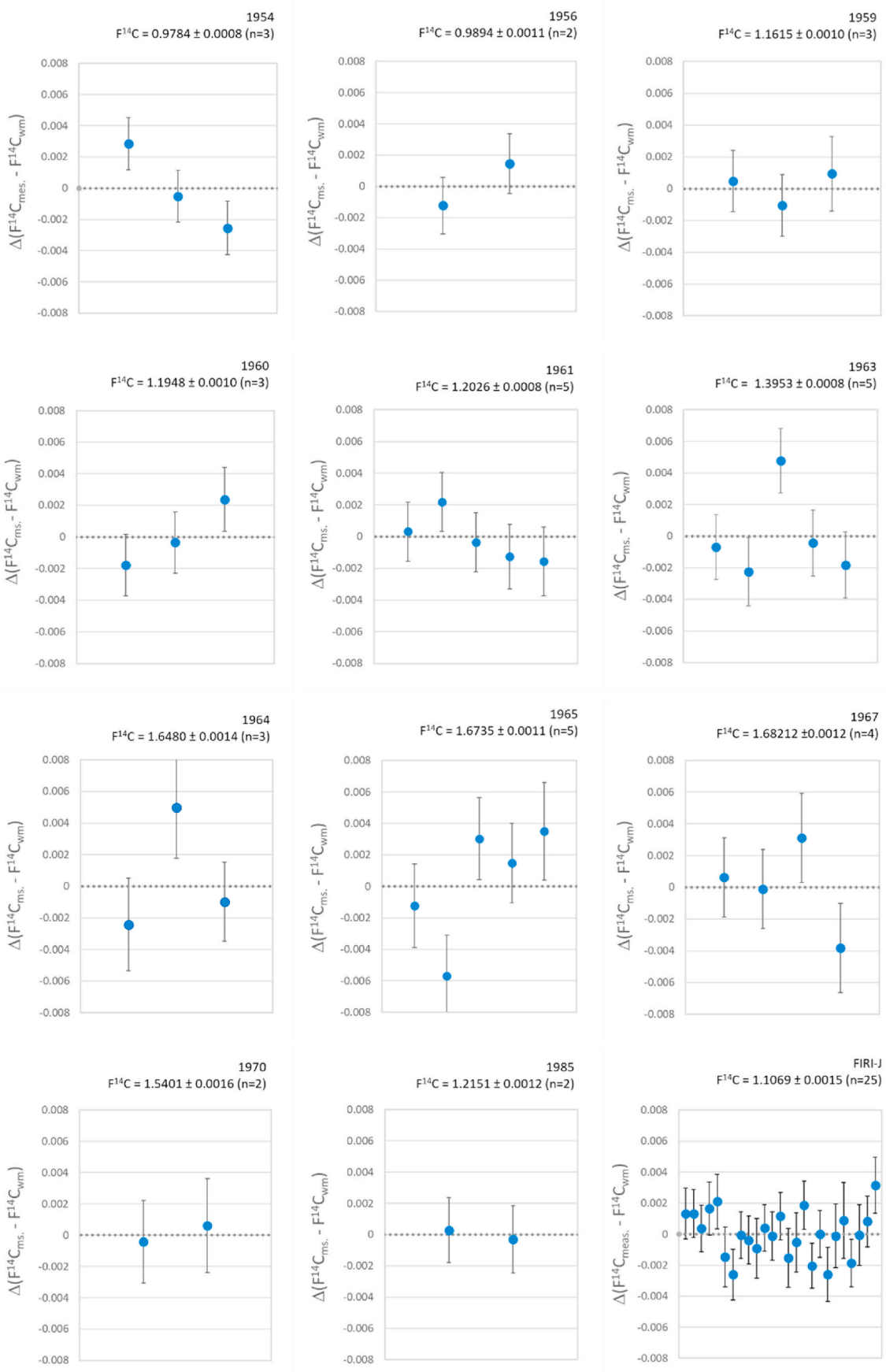

Fig. 7. Radiocarbon values for post-bomb *H. petraeum* of the 11 selected calendar years (36 results in total) as well as those from FIRI-J barley, used as secondary standard on α-cellulose extractions and ^{14}C-AMS measurements. Results include various batches measurement dates.

Table 1
Results of ^{14}C measurements for wood LEN013A *F. cupressoides* series. Measurements were made for wood samples treated using α-cellulose at KCCAMS according to Fig. 3, as well as the CIGA's holocellulose extracts, obtained as described in Southon and Magana (2010). All samples were converted into graphite at KCCAMS, and measured in the same spectrometer. For background corrections we used ^{14}C-free woods, AR2, subject to the same chemical treatments as the late Holocene samples.

Sample name[a]	UCIAMS#	Dated material	$F^{14}C$	±	^{14}C age (yrs BP)	±	Avg. of dupl.	St. dev. of dupl.
LEN013A-003W 438-442CE	255,222	α-cellulose	0.8176	0.0010	1620	15	1623	4
	255,223	α-cellulose	0.8170	0.0011	1625	15		
	253,653	holocellulose	0.8181	0.0014	1615	15		
LEN013A-004W 433-437CE	255,224	α-cellulose	0.8162	0.0013	1630	15		
	253,654	holocellulose	0.8180	0.0013	1615	15	1620	7
	253,671	holocellulose	0.8170	0.0015	1625	15		
LEN013A-008W 413-417CE	255,226	α-cellulose	0.8094	0.0010	1700	15		
	253,658	holocellulose	0.8096	0.0013	1695	15	1685	14
	253,672	holocellulose	0.8116	0.0013	1675	15		
LEN013A-013W 388-392CE	255,227	α-cellulose	0.8074	0.0010	1720	15	1720	0
	255,228	α-cellulose	0.8074	0.0012	1720	15		
	253,673	holocellulose	0.8080	0.0013	1715	15		
LEN013A-017W 368-372CE	255,230	α-cellulose	0.8068	0.0011	1725	15		
	253,667	holocellulose	0.8032	0.0013	1760	15	1738	32
	253,674	holocellulose	0.8078	0.0013	1715	15		

[a] Each LENO13A - sample was processed in triplicate using different chemical extractions; dupl. – short for duplicate.

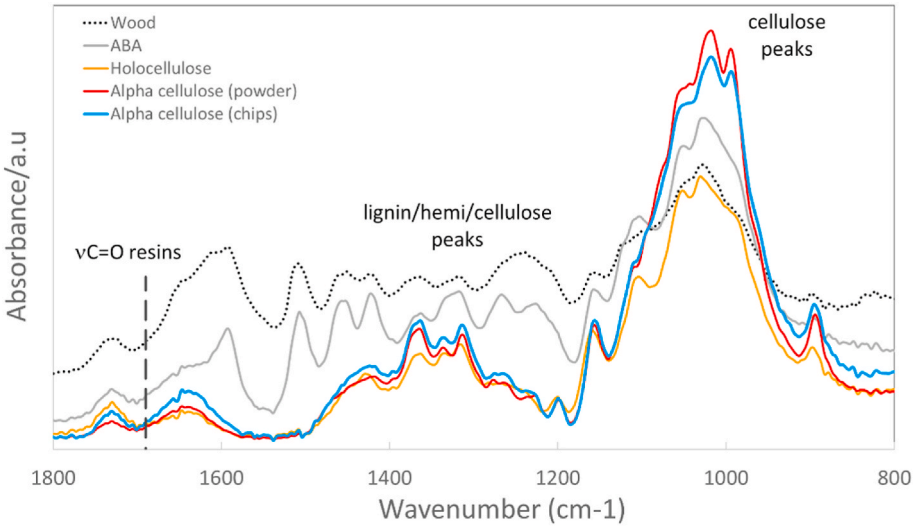

Fig. 8. FTIR spectra of the parenchyma-rich *H. petraeum* samples subjected to the chemical preparation methods ABA, holocellulose, and α-cellulose (cf. Fig. 3), using a single batch of wood reduced to ≤250 μm particles. Spectra of untreated wood and α-cellulose fibers extracted on a separate occasion directly from reduced chips are also shown. Wavenumber for stretching vibrations associated with resins is indicated, as well as main regions where most aromatic rings of lignin, hemicellulose, and cellulose tend to happen. For a better visualization of the aromatic lignin, hemicellulose, and cellulose region, the spectral range was reduced to 1800 to 800 cm^{-1}. This wavelength range corresponds to the region where many soluble wood compounds are found, and can be chemically removed once treatment reach completion.

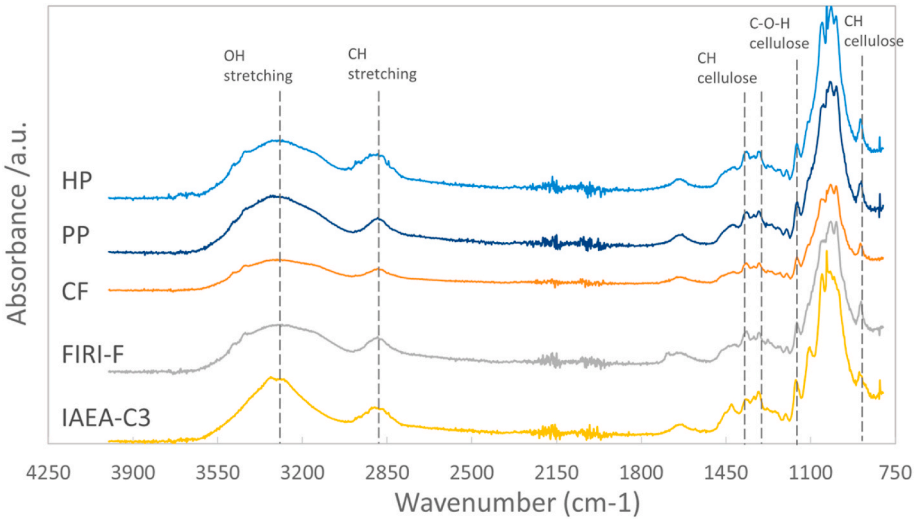

Fig. 9. For visualization's sake, individual α-cellulose spectrum associated with samples are shifted vertically from reference cellulose IAEA-C3 spectrum. CF = *C. fissilis*, PP = *P. paniculata* (those are tropical tree species reported in Santos et al., 2021), and HP = *H. petraeum* (this study). Here, the full spectral range is shown except for the region below 200 cm^{-1} to avoid the noise at the low wavenumber end of each spectrum.

wood samples are rich in extractive substances, such as terpenoids and steroids, waxes, fats, and phenolics (Willför et al., 2003; Pinto et al., 2018). Here, we also showed that our extraction method (cf. Fig. 3) can remove resins from Belfast pine FIRI-F (*Pinus sylvestris* L.) (Fig. 9). Pine woods are known to be highly resinous (≤10% by dry-weight of wood), as shown by the FTIR spectra of untreated whole wood in Rinne et al. (2005).

The procedure's high success rate in organic extractive removal (Fig. 8) may be attributed to the cycling of 1N acid-base-acid treatments at 70 °C, of the standard ABA treatment. Treating plant material with warm diluted acid hydrolysis is known to help to remove organic extractives and soluble sugars, as well as to condition lignin (Pingali et al., 2010). Moreover, experiments in sub-fossil woods (Gillespie, 2019; Van der Wal 2021) and ^{14}C pantropical tree species (Hadad et al., 2015; Baker et al., 2017; Linares et al., 2017; Beramendi-Orosco et al., 2018; Santos et al., 2015, 2020, 2021; Ancapichún et al., 2021) have shown that removal of extractives with organic solvents is not paramount for accurate ^{14}C results. Thus, our analysis, as well as holocellulose extracts conducted by CIGA, have excluded organic solvent treatments for obtaining cellulosic extracts. Second, the application of diluted NaOH to woody parts before the bleaching stage allows for the initiation of delignification, where the bonds between the lignin and the carbohydrates can be weakened (Lehto and Alén 2015). For the remaining portion of our α-cellulose method, the bleaching procedure did not also differ significantly from others, except for the removal of glacial acetic acid as a buffer to activate the chlorite solution. As suggested by Southon and Magana (2010), we replaced this carbon-containing buffer by equal volumes of 1N HCl and 1M $NaClO_2$ solution during complete delignification. We also adopted the alkaline extraction step of 17% (weight/-volume) NaOH for 1 h at room temperature for hemicellulose removal (Oh et al., 2005), and the 1N HCl treatment at 70 °C afterwards before water washes. However, our procedure differs from Southon and Magana (2010) in many ways. We kept sample sizes between 10 and 30 mg per test tube treated (except for blanks and barley, where 40 mg was allowed), so that the total bleaching time could be reduced to less than 3 h. Studies carried out by others had already demonstrated that an extended bleaching duration time beyond 3 h is unnecessary to reach complete delignification (Fogtmann-Schulz et al., 2021). In our case, delignification completion was determined when the reaction (bubbling) stopped, and by the visual inspection of the holocellulose extracts (whiteness level). Both seem to be effective means of determining reaction duration, as demonstrated by the FTIR spectra of the final products (Figs. 8 and 9). We also introduced an additional 1N HCl rinse, just after the 1:1 mixture of 1N HCl and 1M $NaClO_2$ (bleaching), to help on completely remove Cl_2 residues, as well as create a stopping point for leaving samples to rest overnight at room temperature.

More extreme variations included the replacement of the freeze-vacuum-drying step by heat-block-drying overnight, which allowed us to obtain smaller ^{14}C data variations, especially for the ^{14}C-free α-cellulose AVR and AR2 results (Fig. 4). Other important changes were attentive wood cutting before starting chemical extractions (Fig. 2; S1 video - supplementary data) and homogenization of cellulose bundles toward the end of the procedure (Fig. 3). Both steps allowed us to repeatedly obtain accurate and precise radiocarbon dating results of α-cellulose extracts of post-bomb *H. petraeum* tree rings (Fig. 6), as well as from other tropical tree species (Santos et al., 2021), including from the calendar years with the highest variations of atmospheric ^{14}C. Moreover, our chemical procedure seems to handle extremely well with the isolation of structural carbon from woods with abundant parenchyma cells. Such structures (Fig. 1) are known to store nonstructural carbon compounds (Plavcová and Jansen 2015), which can be older than wood stem tissue (Richardson et al., 2013). In this study, we also removed several unwanted wood compounds (Fig. 8), including phenolics. *P. paniculata* tree species, reported in Santos et al. (2021) and FTIR analyzed here (Fig. 9), are known to be loaded with phenolic compounds, which gives it a natural rosacea timber coloration. In order to strip these compounds, first acid treatment of ABA (Fig. 3) was repeated until the supernatant moved from bright-pink (Fig. S2) to clear. As a result, both FTIR spectra (Fig. 9) and ^{14}C results (reported in Santos et al., 2021) were in alignment with expected values of pure α-cellulose extracts.

The simplicity of this hand-operated procedure, which relies on individual test tubes, also allows for some flexibility and adjustments. The wet chemical procedure can be carried on for only a single day, or it can be spread out into two or three days (Fig. 3). No differences in extract quality and/or ^{14}C results were found according to the way sample batches were produced. A hand-operated method may be deemed a limiting factor. But the freedom to adjust loaded batches and chemical volumes up or down as desired avoids the wait for an exact number of samples to begin the procedure. Since this protocol relies mostly on off-the-shelf purified-grade chemicals and the use of single-use (disposable) items, the steps associated with pre-cleaning and sterilizing materials are minimized. Individual test tubes prevent cross-contamination and provide ^{14}C quality assurance. We can conclude that we have perfected a simpler, straightforward, but robust unique protocol that can secure high-quality α-cellulose extracts for ^{14}C analysis of several types of woods of different ages, including tropical trees. Small modifications ensured better background ^{14}C results, as well as remarkably accurate and precise results for post-bomb single tree rings.

4.6. *Implications for tropical tree-ring atmospheric ^{14}C reconstructions and beyond*

Many ongoing efforts to optimize the ^{14}C timescale have allowed researchers to produce calibration curves beyond 50 cal kyr BP (Hogg et al., 2020; Reimer et al., 2020; Hua et al., 2022). Since just a few biological materials can reliably accumulate annual layers (e.g., tree rings, varves, corals, speleothems; Hughen et al., 2004) to help extend the atmospheric ^{14}C time series, dendrochronologically dated tree rings still dominate the development and improvement of ^{14}C calibration curves. To this end, measurements of ^{14}C in tree rings have been taken routinely within five years to the decadal scale (i.e., 5- or 10-year ring measurements) for tree-ring/^{14}C chronologies beyond 1950 AD, while single tree-ring measurements have been mostly used for the post-1950 AD period. Recently, several 1-year ring measurements have been also produced from portions of the pre-1950 AD period to better understand extremely rapid fluctuations in the ^{14}C record in association with astrophysical phenomena (Miyake et al., 2012, 2017; Jull et al., 2014; Güttler et al., 2015; Park et al., 2017; Wang et al., 2017), and/or just for the sake of improving the identification of the ages of significant events (Friedrich et al., 2020), or to increase the robustness of existing datasets (Pearson et al., 2020). As a refinement of such single tree ring ^{14}C measurements, researchers have been proposing to measure just one wood fraction (e.g., late wood - Pearson et al., 2020). The difference between early and late wood may be known as intra-annual, or sub-annual variability, and may result from atmospheric changes or stored carbon (Grootes et al., 1989; Pilcher 1995; Robertson et al., 1997). Intra-annual variability may also be affected by tree species and environmental factors (Kudsk et al., 2018). It is also worth noting that to prevent the influence of old ^{14}C storage in tree rings, α-cellulose fractions should be preferentially used for ^{14}C measurements (Kudsk et al., 2018; Santos et al., 2021, 2022). However, early versus late wood ^{14}C measurements have been limited to few tree species in the extra tropics (Kudsk et al., 2018; Pearson et al., 2020), and insufficient statistical information (e.g., data replication – McDonald et al., 2019).

Until further data can be compiled from multiple tree-species and locations, ^{14}C measurements of whole single tree rings when investigating ^{14}C reconstructions or industrial effects are preferable (see suggestions in Hua et al., 2022). As we demonstrated here, high levels of replication/precision can be obtained from whole rings, so that wood composition variability is insignificant relative to the true atmospheric isotopic signal from when the photosynthates were formed and stored.

This was possible due to: i) careful separation of whole tree rings from wood cross-sections or increment-core (Santos et al., 2021, for example), followed by ii) evaluation under microscopy (to assure growing season uniformity) before reducing them to wood chips (Fig. 2), and iii) extraction to α-cellulose microfibers by a rigorously tested procedure supported with large numbers of all kinds of reference materials and ^{14}C-free samples.

While tropical tree-ring atmospheric ^{14}C reconstructions is still in its infancy compared to the extra tropic works, high levels of replication/precision (Figs. 6 and 7) can be obtained when the precautions mentioned above are applied. As such, a full sequence of 63 single tree rings from 1938 to 2007 from *H. petraeum* tree species found at 1°S, 56°W has been recently measured by ^{14}C (122 results in total) and published in Santos et al. (2022). Fifty-six of the ^{14}C results reported were obtained using the α-cellulose microfibers procedure described in Fig. 3, with the remaining results using extracts from another procedure, as an interlaboratory approach (standard deviation of 0.3%). In Santos et al. (2021), post-1950 AD tree ring ^{14}C results pertaining to 6 calendar years among 7, but from coexisting tree species from sites separated by less than 10 km (e.g., *C. fissilis* and *P. paniculata)*, ^{14}C values were within ±2σ of each other. It seems that our protocol allows us to precisely capture local atmospheric $^{14}CO_2$ distributions, even when we utilize tree species with lifecycles that are most likely slightly misaligned. These examples reinforced the findings of the present study, and will help us move forward on mapping past and present-day $^{14}CO_2$ distribution in trees in places where air-sampling stations are not available.

This is rather important, as currently there is still little data to better define intrahemispheric offsets, which define the geographical division of the most recent ^{14}C atmospheric timescale (i.e., the last 70 years; Hua et al., 2022). Further tree ring atmospheric ^{14}C reconstructions across distinct latitudinal and longitudinal regions will helps us evaluate future changes: e.g., how atmospheric circulation may change as the climate warms and how trees will cope under extreme climatic conditions. We believe that our method can help to expedite the production of new ^{14}C records.

5. Conclusions

Findings from our study, which is based on a statistically significant number of measurements, demonstrate that a universal α-cellulose procedure can be applied with high degrees of reliability from wood materials ranging from the ^{14}C limit to the post-bomb era. In sum, our procedure repeatedly yields accurate and precise ^{14}C results, regardless of wood types, myriads of natural wood extractives, varying loads and allocations of labile carbon in wood cells, and most importantly, their ^{14}C age group. Radiocarbon results from cellulosic extracts were on the order of 0.2% based on a simple pooled standard deviation calculation. Nonetheless, we chose to quote an accuracy/precision of 0.29% to include the standard deviations of measurements of organic combustibles (OX-IIs and ANUs), which were measured with cellulosic samples for spectrometer quality control.

The chemical procedure for isolating cellulose per se is not very different from other simpler treatments already described in the literature. Nonetheless, the success of the improved procedure has been attributed to modifications both before and after chemical treatment takes place. Special attention has been given to tree-ring dissection and wood sample preparation before the chemical procedure is applied, to microfiber homogenization upon α-cellulose extraction, and to microfiber drying, so that high-quality and reliable results can be obtained. Our results also support previous studies indicating that solvent extraction prior to chemical bleaching during cellulose extraction can be suppressed. Moreover, this procedure is very versatile and inclusive. It can be easily scaled up or down and/or modified on demand (i.e., steps can be easily added or removed, depending on wood sample specifications).

Here, we demonstrate very small differences in ^{14}C signatures within a growing season through replication of results. Therefore, we feel that our simpler and straightforward α-cellulose procedure would benefit the scientific community by providing faithful signatures of past atmospheric $^{14}CO_2$ variations as well carbon isotopic analysis for a variety of studies.

Credit authorship contribution statementse

Guaciara M. Santos: Conceptualization, Project administration, Funding acquisition, Radiocarbon methodology, Supervision, Investigation, Formal analysis and interpretation, Writing - original draft, Writing - review & editing, visualization, data curation, validation, literature synthesis, and discussion. **Anita S.Y. Komatsu:** Cellulose extraction methodology, Radiocarbon sample processing and data analysis, Writing – original draft, visualization, literature synthesis and discussion. **Jazmine M. Renteria Jr.:** Cellulose extraction methodology. Radiocarbon sample processing. **Arno Fritz das Neves Brandes:** Tree-ring Methodology, Writing - review & editing, literature synthesis and discussion. **Christopher A. Leong:** FTIR analysis, visualization and interpretation, Writing - review & editing. **Silvana Collado-Fabbri:** Cellulose extraction methodology at CIGA. **Ricardo De Pol-Holz:** Writing - review & editing, literature synthesis and discussion.

Declaration of competing interest

The authors declare that they have no known competing financial interests or personal relationships that could have appeared to influence the work reported in this paper.

Data availability

Data will be made available on request.

Acknowledgements

This research was supported by the United States National Science Foundation to G.M.S. (AGS-1903690 and AGS-1703035). R.D.P-H. was supported by Fondecyt grant 1201810. G.M.S and C.A.L. thank Jovany Merham, Evan Patrick Garcia, and Dr. Dima Fishman from the Laser Spectroscopy Labs, University of California, Irvine, for assistance on FTIR acquisition. We sincerely thank the anonymous reviewers and editor.

Appendix A. Supplementary data

Supplementary data to this article can be found online at https://doi.org/10.1016/j.quageo.2022.101414.

References

Aguayo, M.G., Fernández Pérez, A., Reyes, G., Oviedo, C., Gacitúa, W., Gonzalez, R., Uyarte, O., 2018. Isolation and characterization of cellulose nanocrystals from rejected fibers originated in the kraft pulping process. Polymers 10 (10), 1145.

Ancapichún, S., De Pol-Holz, R., Christie, D.A., Santos, G.M., Collado-Fabbri, S., Garreaud, R., Lambert, F., Orfanoz-Cheuquelaf, A., Rojas, M., Southon, J., Turnbull, J.C., 2021. Radiocarbon bomb-peak signal in tree-rings from the tropical Andes register low latitude atmospheric dynamics in the Southern Hemisphere. Sci. Total Environ. 774, 145126 https://doi.org/10.1016/j.scitotenv.2021.145126.

Anchukaitis, K.J., Evans, M.N., Lange, T., Smith, D.R., Leavitt, S.W., Schrag, D.P., 2008. Consequences of a rapid cellulose extraction technique for oxygen isotope and radiocarbon analyses. Anal. Chem. 80 (6), 2035–2041.

Andreu-Hayles, L., Levesque, M., Martin-Benito, D., Huang, W., Harris, R., Oelkers, R., Leland, C., Martin-Fernández, J., Anchukaitis, K.J., Helle, G., 2019. A high yield cellulose extraction system for small whole wood samples and dual measurement of carbon and oxygen stable isotopes. Chem. Geol. 504, 53–65.

Baker, J.C.A., Santos, G.M., Gloor, M., Brienen, R.J.W., 2017. Does Cedrela always form annual rings? Testing ring periodicity across South America using radiocarbon dating. Trees (Berl.). https://doi.org/10.1007/s00468-017-1604-9.

Beramendi-Orosco, L.E., Johnson, K.R., Noronha, A.L., González-Hernández, G., Villanueva-Díaz, J., 2018. High precision radiocarbon concentrations in tree rings

from Northeastern Mexico: a new record with annual resolution for dating the recent past. Quat. Geochronol. 48, 1–6. https://doi.org/10.1016/j.quageo.2018.07.007.
Beverly, R.K., Beaumont, W., Tauz, D., Ormsby, K.M., von Reden, K.F., Santos, G.M., Southon, J.R., 2010. The Keck carbon cycle AMS laboratory, university of California, irvine: status report. Radiocarbon 52 (2), 301–309.
Brock, F., Dee, M., Hughes, A., Snoeck, C., Staff, R., Ramsey, C.B., 2018. Testing the effectiveness of protocols for removal of common conservation treatments for radiocarbon dating. Radiocarbon 60 (1), 35–50.
Capano, M., Miramont, C., Guibal, F., Kromer, B., Tuna, T., Fagault, Y., Bard, E., 2018. Wood 14C dating with AixMICADAS: methods and application to tree-ring sequences from the Younger Dryas Event in the southern French Alps. Radiocarbon 60 (1), 51–74.
Cercatillo, S., Friedrich, M., Kromer, B., Paleček, D., Talamo, S., 2021. Exploring different methods of cellulose extraction for 14 C dating. New J. Chem. 45 (20), 8936–8941.
Danišík, M., Shane, P., Schmitt, A.K., Hogg, A., Santos, G.M., Storm, S., Evans, N.J., Fifield, L.K., Lindsay, J.M., 2012. Re-anchoring the late Pleistocene tephrochronology of New Zealand based on concordant radiocarbon ages and combined 238U/230Th disequilibrium and (U–Th)/He zircon ages. Earth Planet Sci. Lett. 349, 240–250.
Dee, M.W., Brock, F., Bowles, A.D., Ramsey, C.B., 2011. Using a silica substrate to monitor the effectiveness of radiocarbon pretreatment. Radiocarbon 53 (4), 705–711.
Dee, M.W., Palstra, S.W.L., Aerts-Bijma, A.T., Bleeker, M.O., De Bruijn, S., Ghebru, F., Jansen, H.G., Kuitems, M., Paul, D., Richie, R.R., Spriensma, J.J., 2020. Radiocarbon dating at Groningen: new and updated chemical pretreatment procedures. Radiocarbon 62 (1), 63–74.
Fogtmann-Schulz, A., Kudsk, S.G., Adolphi, F., Karoff, C., Knudsen, M.F., Loader, N.J., Muscheler, R., Trant, P.L., Østbø, S.M., Olsen, J., 2021. Batch processing of tree-ring samples for radiocarbon analysis. Radiocarbon 63 (1), 77–89. https://doi.org/10.1017/RDC.2020.119.
Friedrich, R., Kromer, B., Wacker, L., Olsen, J., Remmele, S., Lindauer, S., Land, A., Pearson, C., 2020. A new annual 14C dataset for calibrating the Thera eruption. Radiocarbon 62 (4), 953–961.
Gaudinski, J.B., Dawson, T.E., Quideau, S., Schuur, E.A.G., Roden, J.S., Trumbore, S.E., Sandquist, D.R., Oh, S.-W., Wasylishen, R.E., 2005. Comparative analysis of cellulose preparation techniques for use with 13C, 14C and 18O isotopic measurements. Anal. Chem. 77 (22), 7212–7224.
Gillespie, R., 2019. A novel cellulose-preparation method. Radiocarbon 61 (1), 131–139. https://doi.org/10.1017/RDC.2018.65.
Groenendijk, P., Sass-Klaassen, U., Bongers, F., Zuidema, P.A., 2014. Potential of tree-ring analysis in a wet tropical forest: a case study on 22 commercial tree species in Central Africa. For. Ecol. Manag. 323, 65–78.
Grootes, P.M., Farwell, G.W., Schmidt, F.H., Leach, D.D., Stuiver, M., 1989. Rapid response of tree cellulose radiocarbon content to changes in atmospheric 14; CO2 concentration. Tellus B 41 (2), 134–148.
Güttler, D., Adolphi, F., Beer, J., Bleicher, N., Boswijk, G., Christl, M., Hogg, A., Palmer, J., Vockenhuber, C., Wacker, L., Wunder, J., 2015. Rapid increase in cosmogenic 14C in AD- 775 measured in New Zealand kauri trees indicates short-lived increase in 14C production spanning both hemispheres. Earth Planet Sci. Lett. 411, 290–297.
Hadad, M.A., Santos, G.M., Juñent, F.A.R., Grainger, C.S., 2015. Annual nature of the growth rings of Araucaria araucana confirmed by radiocarbon analysis. Quat. Geochronol. 30, 42–47. https://doi.org/10.1016/j.quageo.2015.05.002.
Hajdas, I., Hendriks, L., Fontana, A., Monegato, G., 2017. Evaluation of preparation methods in radiocarbon dating of old wood. Radiocarbon 59 (3), 727–737.
Hartmann, H., Trumbore, S., 2016. Understanding the roles of nonstructural carbohydrates in forest trees–from what we can measure to what we want to know. New Phytol. 211 (2), 386–403.
Hogg, A.G., 2004. Towards achieving low background levels in routine dating by liquid scintillation spectrometry. Radiocarbon 46 (1), 123–131. https://doi.org/10.1017/S0033822200039436.
Hogg, A., Heaton, T.J., Hua, Q., Palmer, J.G., Turney, C.S.M., Southon, J., Bayliss, A., Blackwell, P.G., Boswijk, G., Bronk Ramsey, C., Pearson, C., Petchey, F., Reimer, P., Reimer, R., Wacker, L., 2020. SHCal20 Southern Hemisphere calibration, 0-55,000 years cal BP. Radiocarbon 62 (4), 759–778. https://doi.org/10.1017/RDC.2020.59.
Hua, Q., Barbetti, M., 2004. Review of tropospheric bomb radiocarbon data for carbon cycle modeling and age calibration purposes. Radiocarbon 46 (3), 1273–1298.
Hua, Q., Barbetti, M., Jacobsen, G., Zoppi, U., Lawson, E., 2000. Bomb radiocarbon in annual tree rings from Thailand and Australia. Nucl. Instrum. Methods Phys. Res. B 172 (1–4), 359–365.
Hua, Q., Barbetti, M., Rakowski, A.Z., 2013. Atmospheric radiocarbon for the period 1950–2010. Radiocarbon 55 (4), 2059–2072. https://doi.org/10.2458/azu_js_rc.v55i2.16177.
Hua, Q., Turnbull, J.C., Santos, G.M., Rakowski, A.Z., Ancapichún, S., De Pol-Holz, R., Hammer, S., Lehman, S.J., Levin, I., Miller, J.B., Palmer, J.G., 2022. Atmospheric radiocarbon for the period 1950–2019. Radiocarbon 64 (4), 723–745. https://doi.org/10.1017/RDC.2021.95.
Hughen, K., Lehman, S., Southon, J., Overpeck, J., Marchal, O., Herring, C., Turnbull, J., 2004. 14C activity and global carbon cycle changes over the past 50,000 years. Science 303 (5655), 202–207.
Jull, A.J., Panyushkina, I.P., Lange, T.E., Kukarskih, V.V., Myglan, V.S., Clark, K.J., Salzer, M.W., Burr, G.S., Leavitt, S.W., 2014. Excursions in the 14C record at AD 774–775 in tree rings from Russia and America. Geophys. Res. Lett. 41 (8), 3004–3010. https://doi.org/10.1002/2014GL059874.
Jull, A.J.T., Pearson, C.L., Taylor, R.E., Southon, J.R., Santos, G.M., Kohl, C.P., Hajdas, I., Molnar, M., Baisan, C., Lange, T.E., Cruz, R., 2018. Radiocarbon dating and intercomparison of some early historical radiocarbon samples. Radiocarbon 60 (2), 535–548.
Kudsk, S.G., Olsen, J., Nielsen, L.N., Fogtmann-Schulz, A., Knudsen, M.F., Karoff, C., 2018. What is the carbon origin of early-wood? Radiocarbon 60 (5), 1457–1464.
Kutschera, W., 2020. On the enigma of dating the Minoan eruption of Santorini. Proc. Natl. Acad. Sci. USA 117 (16), 8677–8679.
Lange, T.E., Nordby, J.A., Murphy, P.L.O., Hodgins, G.W.L., Pearson, C.L., 2019. A detailed investigation of pretreatment protocols for high precision radiocarbon measurements of annual tree-rings. Nucl. Instrum. Methods Phys. Res. Sect. B Beam Interact. Mater. Atoms 455, 230–233.
Lara, A., Villalba, R., Urrutia-Jalabert, R., González-Reyes, A., Aravena, J.C., Luckman, B. H., Cuq, E., Rodríguez, C., Wolodarsky-Franke, A., 2020. +A 5680-year tree-ring temperature record for southern South America. Quat. Sci. Rev. 228 https://doi.org/10.1016/j.quascirev.2019.106087.
Laumer, W., Andreu, L., Helle, G., Schleser, G.H., Wieloch, T., Wissel, H., 2009. A novel approach for the homogenization of cellulose to use micro-amounts for stable isotope analyses. Rapid Commun. Mass Spectrom.: An International Journal Devoted to the Rapid Dissemination of Up-to-the-Minute Research in Mass Spectrometry 23 (13), 1934–1940.
Lehto, J., Alén, R., 2015. Chemical pretreatments of wood chips prior to alkaline pulping: a review of pretreatment alternatives, chemical aspects of the resulting liquors, and pulping outcomes. Bioresources 10 (4), 8604–8656. https://doi.org/10.15376/biores.10.4.lehto.
Linares, R., Santos, H.C., Brandes, A.F.N., Barros, C.F., Lisi, C.S., Balieiro, F.C., de Faria, S.M., 2017. Exploring the 14C bomb peak with tree rings of tropical species from the Amazon forest. Radiocarbon 59 (2), 303–313. https://doi.org/10.1017/RDC.2017.10.
McDonald, L., Chivall, D., Miles, D., Bronk Ramsey, C., 2019. Seasonal variations in the 14 C content of tree rings: influences on radiocarbon calibration and single-year curve construction. Radiocarbon 61, 185–194. https://doi.org/10.1017/RDC.2018.64.
Michczyńska, D.J., Krąpiec, M., Michczyński, A., Pawlyta, J., Goslar, T., Nawrocka, N., Piotrowska, N., Szychowska-Krąpiec, E., Waliszewska, B., Zborowska, M., 2018. Different pretreatment methods for 14C dating of Younger Dryas and Allerød pine wood (Pinus sylvestris L.). Quat. Geochronol. 48, 38–44.
Miyake, F., Nagaya, K., Masuda, K., Nakamura, T., 2012. A signature of cosmic-ray increase in AD 774–775from tree rings in Japan. Nature 486, 240–2.
Miyake, F., Jull, A.T., Panyushkina, I.P., Wacker, L., Salzer, M., Baisan, C.H., Lange, T., Cruz, R., Masuda, K., Nakamura, T., 2017. Large 14C excursion in 5480 BC indicates an abnormal sun in the mid-Holocene. Proc. Natl. Acad. Sci. U.S.A. 114, 881–884.
Mook, W.G., Van der Plicht, J., 1999. Reporting 14C activities and concentrations. Radiocarbon 41 (3), 227–239.
Morris, H., Brodersen, C., Schwarze, F.W., Jansen, S., 2016. The parenchyma of secondary xylem and its critical role in tree defense against fungal decay in relation to the CODIT model. Front. Plant Sci. 7, 1665.
Oh, S.Y., Yoo, D.I., Shin, Y., Kim, H.C., Kim, H.Y., Chung, Y.S., Park, W.H., Youk, J.H., 2005. Crystalline structure analysis of cellulose treated with sodium hydroxide and carbon dioxide by means of X-ray diffraction and FTIR spectroscopy. Carbohydr. Res. 340 (15), 2376–2391.
Ostapkowicz, J., Ramsey, C.B., Brock, F., Higham, T., Wiedenhoeft, A.C., Ribechini, E., Lucejko, J.J., Wilson, S., 2012. Chronologies in wood and resin: AMS 14C dating of pre-Hispanic Caribbean wood sculpture. J. Archaeol. Sci. 39 (7), 2238–2251.
Park, J., Southon, J., Fahrni, S., Creasman, P.P., Mewaldt, R., 2017. Relationship between solar activity and Δ14C peaks in AD 775, AD 994, and 660 BC. Radiocarbon 59 (4), 1147–1156.
Pearson, C., Wacker, L., Bayliss, A., Brown, D., Salzer, M., Brewer, P., Bollhalder, S., Boswijk, G., Hodgins, G., 2020. Annual variation in atmospheric 14C between 1700 BC and 1480 BC. Radiocarbon 62 (4), 939–952.
Pilcher, J.R., 1995. Biological considerations in the interpretation of stable isotope ratios in oak tree- rings. In: Frinzel, B., Stauffer, B., Weiss, M.M. (Eds.), Paläoklimaforschung/Paleoclimate Research 15, 157–161.
Pingali, S.V., Urban, V.S., Heller, W.T., McGaughey, J., O'Neill, H., Foston, M., Myles, D. A., Ragauskas, A., Evans, B.R., 2010. Breakdown of cell wall nanostructure in dilute acid pretreated biomass. Biomacromolecules 11 (9), 2329–2335.
Pinto, R.B., Lusa, M.G., Mansano, V.D.F., Tozzi, A.M.G.D.A., Mayer, J.L.S., 2018. Morphoanatomy of the leaflets of the Hymenaea clade (Fabaceae: detarioideae) reveals their potential for taxonomic and phylogenetic studies. Bot. J. Linn. Soc. 187 (1), 87–98.
Plavcová, L., Jansen, S., 2015. The role of xylem parenchyma in the storage and utilization of nonstructural carbohydrates. In: Hacke, U. (Ed.), Functional and Ecological Xylem Anatomy. Springer International, Cham, Switzerland, pp. 209–234. https://doi.org/10.1007/978-3-319-15783-2_8.
Reimer, P.J., Brown, T., Reimer, R.W., 2004. Discussion: reporting and calibration of post-bomb 14C data. Radiocarbon 46, 1299–1304.
Reimer, P.J., Austin, W.E., Bard, E., Bayliss, A., Blackwell, P.G., Ramsey, C.B., Butzin, M., Cheng, H., Edwards, R.L., Friedrich, M., Grootes, P.M., 2020. The IntCal20 Northern Hemisphere radiocarbon age calibration curve (0–55 cal kBP). Radiocarbon 62 (4), 725–757. https://doi.org/10.1017/RDC.2020.41.
Richard, B., Quilès, F., Carteret, C., Brendel, O., 2014. Infrared spectroscopy and multivariate analysis to appraise α-cellulose extracted from wood for stable carbon isotope measurements. Chem. Geol. 381, 168–179.
Richardson, A.D., Carbone, M.S., Keenan, T.F., Czimczik, C.I., Hollinger, D.Y., Murakami, P., Schaberg, P.G., Xu, X.M., 2013. Seasonal dynamics and age of

stemwood nonstructural carbohydrates in temperate forest trees. New Phytol. 197, 850–861. https://doi.org/10.1111/nph.12042.

Rinne, K.T., Boettger, T., Loader, N.J., Robertson, I., Switsur, V.R., Waterhouse, J.S., 2005. On the purification of alpha-cellulose from resinous wood for stable isotope (H, C and O) analysis. Chem. Geol. 222 (1–2), 75–82. https://doi.org/10.1016/j.chemgeo.2005.06.010.

Robertson, I., Switsur, V.R., Carter, A.H.C., Barker, A.C., Waterhouse, J.S., Briffa, K.R., Jones, P.D., 1997. Signal strength and climate relationships in 13C/12C ratios of tree ring cellulose from oak in east England. J. Geophys. Res. Atmos. 102 (D16), 19507–19516. https://doi.org/10.1029/97JD01226.

Santos, G.M., Ormsby, K., 2013. Behavioral variability in ABA chemical pretreatment close to the 14C age limit. Radiocarbon 55 (2), 534–544. https://doi.org/10.1017/S0033822200057660.

Santos, G.M., Xu, X., 2017. Bag of tricks: a set of techniques and other resources to help 14C laboratory setup, sample processing, and beyond. Radiocarbon 59 (3), 785–801. https://doi.org/10.1017/RDC.2016.43.

Santos, G.M., Linares, R., Lisi, C.S., Tomazello Filho, M., 2015. Annual growth rings in a sample of Paraná pine (Araucaria angustifolia): toward improving the 14C calibration curve for the Southern Hemisphere. Quat. Geochronol. 25, 96–103. https://doi.org/10.1016/j.quageo.2014.10.004.

Santos, G.M., Granato-Souza, D., Barbosa, A.C., Oelkers, R., Andreu-Hayles, L., 2020. Radiocarbon analysis confirms annual periodicity in Cedrela odorata tree rings from the equatorial Amazon. Quat. Geochronol. 58, 101079.

Santos, G.M., Rodriguez, D.R.O., Barreto, N.D.O., Assis-Pereira, G., Barbosa, A.C., Roig, F.A., Tomazello-Filho, M., 2021. Growth assessment of native tree species from the southwestern Brazilian amazonia by post-AD 1950 14C analysis: implications for tropical dendroclimatology studies and atmospheric 14C reconstructions. Forests 12 (9), 1177. https://doi.org/10.3390/F12091177.

Santos, G.M., Albuquerque, R.P., Barros, C.F., Ancapichún, S., Oelkers, R., Andreu-Hayles, L., de Faria, S.M., De Pol-Holz, R., Brandes, A.F.N., 2022. High-precision 14C measurements of parenchyma-rich *Hymenolobium petraeum* tree species confirm bomb-peak atmospheric levels and reveal local fossil-fuel CO2 emissions in the Central Amazon. Environ. Res. 214 (3), 113994 https://doi.org/10.1016/j.envres.2022.113994.

Scott, E.M., Boaretto, E., Bryant, C., Cook, G.T., Gulliksen, S., Harkness, D.D., Heinemeier, J., McGee, E., Naysmith, P., Possnert, G., van der Plicht, H., 2004. Future needs and requirements for AMS 14C standards and reference materials. Nucl. Instrum. Methods Phys. Res. Sect. B Beam Interact. Mater. Atoms 223, 382–387.

Scott, E., Cook, G., Naysmith, P., Staff, R., 2019. Learning from the wood samples in ICS, TIRI, FIRI, VIRI, and SIRI. Radiocarbon 61 (5), 1293–1304. https://doi.org/10.1017/RDC.2019.12.

Southon, J.R., Magana, A.L., 2010. A comparison of cellulose extraction and ABA pretreatment methods for AMS 14C dating of ancient wood. Radiocarbon 52 (3), 1371–1379.

Spurk, M., Friedrich, M., Hofmann, J., Remmele, S., Frenzel, B., Leuschner, H.H., Kromer, B., 1998. Revisions and extension of the Hohenheim oak and pine chronologies: new evidence about the timing of the Younger Dryas/Preboreal transition. Radiocarbon 40 (3), 1107–1116.

Stuiver, M., Polach, H.A., 1977. Discussion reporting of 14C data. Radiocarbon 19, 355–363.

Stuiver, M., Quay, P.D., 1981. Atmospheric14C changes resulting from fossil fuel CO2 release and cosmic ray flux variability. Earth Planet Sci. Lett. 53 (3), 349–362.

Van der Wal, K.S., 2021. Looking into Contamination in Wood Samples for Radiocarbon Analysis Using FTIR. Centre for Isotope Analysis (CIO), University of Groningen. MSc research project (s4181808). Available online fse.studenttheses.ub.rug.nl.

Wang, F.Y., Yu, H., Zou, Y.C., Dai, Z.G., Cheng, K.S., 2017. A rapid cosmic-ray increase in BC 3372–3371 from ancient buried tree rings in China. Nat. Commun. 8 (1), 1487.

Wieloch, T., Helle, G., Heinrich, I., Voigt, M., Schyma, P., 2011. A novel device for batch-wise isolation of α-cellulose from small-amount wholewood samples. Dendrochronologia 29 (2), 115–117.

Willför, S.M., Ahotupa, M.O., Hemming, J.E., Reunanen, M.H., Eklund, P.C., Sjöholm, R. E., Eckerman, C.S., Pohjamo, S.P., Holmbom, B.R., 2003. Antioxidant activity of know wood extractives and phenolic compounds of selected tree species. J. Agric. Food Chem. 51 (26), 7600–7606.